GEOMECHANICAL MODELING OF SALT CAVERN STABILITY FOR CARBON DIOXIDE
STORAGE IN THE MAHA SARAKHAM FORMATION, NORTHEASTERN THAILAND

Miss Narumas Pajonpai

A Thesis Submitted in Partial Fulfillment of the Requirements

for the Degree of Master of Engineering in Georesources and Petroleum Engineering

Department of Mining and Petroleum Engineering

Faculty of Engineering

Chulalongkorn University

Academic Year 2019

แบบจำลองทางกลศาสตร์ธรณีของความมั่นคงของโพรงเกลือเพื่อเป็นแหล่งกักเก็บคาร์บอนไดออกไซด์
ในหมวดหินมหาสารคามภาคตะวันออกเฉียงเหนือของประเทศไทย

น.ส.นฤมาศ ผจญภัย

Thesis Title	GEOMECHANICAL MODELING OF SALT CAVERN STABILITY FOR CARBON DIOXIDE STORAGE IN THE MAHA SARAK-HAM FORMATION, NORTHEASTERN THAILAND
By	Miss Narumas Pajonpai
Field of Study	Georesources and Petroleum Engineering
Thesis Advisor	Raphael Bissen, Dr.rer.nat.
Thesis Co Advisor	Assistant Professor Sunthorn Pumjan, Ph.D.

Accepted by the Faculty of Engineering, Chulalongkorn University in Partial Fulfillment of the Requirement for the Master of Engineering

.... Dean of the Faculty of Engineering

(Professor SUPOT TEACHAVORASINSKUN, D.Eng.)

THESIS COMMITTEE

.... Chairman

(Assistant Professor JIRAWAT CHEWAROUNGROAJ, Ph.D.)

.... Thesis Advisor

(Raphael Bissen, Dr.rer.nat.)

.... Thesis Co-Advisor

(Assistant Professor Sunthorn Pumjan, Ph.D.)

.... Examiner

(Apisit Numprasanthai, Ph.D.)

.... External Examiner

(Songwut Artittong, Ph.D.)

นฤมาศ ผจญภัย : แบบจำลองทางกลศาสตร์ธรณีของความมั่นคงของโพรงเกลือเพื่อเป็นแหล่งกักเก็บ คาร์บอนไดออกไซด์ในหมวดหินมหาสารคามภาคตะวันออกเฉียงเหนือของประเทศไทย. (GEOMECHANI-CAL MODELING OF SALT CAVERN STABILITY FOR CARBON DIOXIDE STORAGE IN THE MAHA SARAKHAM FORMATION, NORTHEASTERN THAILAND) อ.ที่ปรึกษาหลัก : อ. ดร.ราฟาเอล บิสเซ่น, อ. ที่ปรึกษาร่วม : ผศ. ดร.สุนทร พุ่มจันทร์

ในรอบสามทศวรรษ ประเทศไทยได้ทำการปล่อยก๊าซคาร์บอนไดออกไซด์ (CO_2) เพิ่มขึ้นอย่างต่อเนื่องเป็นสี่เท่าตั้งแต่ปี ค.ศ. 1989 ภาคส่วนการผลิตพลังงานเป็นภาคส่วนหลักที่ทำการปล่อยก๊าซ CO_2 โดยการเผาไหม้เชื้อเพลิงฟอสซิลเพื่อผลิต กระแสไฟฟ้า ดังนั้นอุตสาหกรรมการผลิตพลังงานจึงถูกเพ่งเล็งและถูกกดดันจากสังคมให้แสดงความรับผิดชอบ การดักจับและการ กักเก็บคาร์บอน (Carbon capture and storage : CCS) เป็นหนึ่งในวิธีการที่จะรับมือกับการปล่อยก๊าซ CO_2 โดยทั่วไปการดักจับ และกักเก็บไว้ในโครงสร้างทางธรณีวิทยา เช่น แหล่งหินเกลือ ที่สามารถพบได้หลากหลายภูมิภาคทั่วโลก ซึ่งเป็นผลให้ โพรงเกลือ ได้ ถูกนำมาศึกษาอย่างจริงจังเกี่ยวกับการนำมาใช้กักเก็บ CO_2 เนื่องจากคุณสมบัติที่เหมาะสม ในงานวิจัยนี้ ระเบียบวิธีไฟไนต์เอเล เมนต์ (Finite Element Method : FEM, ANSYS Student 2019 R2) ได้ถูกนำมาใช้เพื่อหารูปร่างที่เหมาะสมของโพรงเกลือที่ สามารถทำเหมืองได้ด้วยวิธีการทำเหมืองละลายในระดับลึก โดยรูปร่างที่นำมาวิเคราะห์ ได้แก่ รูปทรงกลม, รูปหยดน้ำ, รูปแพร์, รูป หลอดไฟ และรูปทรงกระบอก โดยปริมาตรของรูปที่ออกแบบจะมีปริมาตรประมาณ 520,000 ลูกบาศก์เมตร ซึ่งจะสามารถจุ CO_2 ได้ 0.4 ล้านตัน ในสถานะของของไหลวิกฤติยิ่งยวด (Supercritical fluid) ค่าความปลอดภัย และ การลดลงของปริมาตรเป็นเกณฑ์ ในการหารูปร่างของโพรงที่เหมาะสมสำหรับกักเก็บ CO_2 สำหรับพื้นที่ที่ถูกเลือกเพื่อใช้เป็นกรณีศึกษา คือบริเวณโดยรอบของหลุม เจาะ K-89 ที่บ้านหนองปู อำเภอบรบือ จังหวัดมหาสารคาม ในภาคตะวันออกเฉียงเหนือของประเทศไทย เนื่องจากแหล่งปล่อย ก๊าซ CO_2 กับแหล่งกักเก็บ CO_2 อยู่บริเวณใกล้เคียงกัน สำหรับข้อมูลที่นำเข้าไปใช้ในการออกแบบ ได้แก่ รูปร่างเรขาคณิตของโพรง, คุณสมบัติของวัสดุ (ชนิดหิน) และค่าความคืบของหินเกลือ ซึ่งในกรณีศึกษานี้ Norton creep power law ได้ถูกนำมาใช้เพื่อบ่ง บอกอัตราการเปลี่ยนความเครียดต่อช่วงเวลาคงที่ (Steady -state stage of creep) ขั้นตอนการจำลองจะเป็นไปตามกระบวนการ ของการกักเก็บ CO_2 ตั้งแต่การทำเหมืองละลายจนถึงหลังการปิดโพรง 500 ปี ซึ่งผลของการจำลองบ่งบอกว่า การที่ความกว้างของ โพรง ในช่วงหนึ่งในสามของความสูงโพรง ยิ่งกว้าง มีผลต่อการลดลงของปริมาตร โดยความกว้างโพรงยิ่งน้อย การลดลงของ ปริมาตรก็จะน้อยลงตามไปด้วย จากผลของโพรงที่มีความสูงเท่ากัน นอกจากนี้ในทุกรูปร่างของโพรง มีค่าความปลอดภัยมากกว่า 1 ทำให้รูปร่างที่ออกแบบทั้งหมดสามารถนำมาใช้ในการกักเก็บคาร์บอนไดออกไซด์ในภาคตะวันออกเฉียงเหนือของประเทศไทย โดย รูปร่างของโพรงเกลือที่เหมาะสมที่สุดที่ทำให้โพรงเกลือมีเสถียรภาพมากที่สุดคือ รูปหยดน้ำ โดยมีค่าความปลอดภัย อยู่ที่ 6.36 และ มีการลดลงของปริมาตรน้อยที่สุด (0.018%) จากบรรดาทุกรูปที่ออกแบบ

สาขาวิชา	วิศวกรรมทรัพยากรธรณีและ ปิโตรเลียม	ลายมือชื่อนิสิต ....
ปีการศึกษา	2562	ลายมือชื่อ อ.ที่ปรึกษาหลัก ....
		ลายมือชื่อ อ.ที่ปรึกษาร่วม ....

6071204021 : MAJOR GEORESOURCES AND PETROLEUM ENGINEERING

Narumas Pajonpai : GEOMECHANICAL MODELING OF SALT CAVERN STABILITY FOR CARBON DIOXIDE STORAGE IN THE MAHA SARAKHAM FORMATION, NORTHEASTERN THAILAND. Advisor: Raphael Bissen, Dr.rer.nat. Co-advisor: Asst. Prof. Sunthorn Pumjan, Ph.D.

In Thailand, CO_2 emissions quadrupled over the past three decades since 1989, with the power generation sector as the main contributor by burning fossil fuels to produce electricity. Therefore, the power generating industry has come under scrutiny and been pressed by society to take responsibility. Carbon Capture and Storage (CCS) is one of the many methods to deal with CO_2 emissions. Generally, CO_2 is captured and stored in geological formations, e.g. rock salt deposits. Salt caverns have been intensively studied regarding their usage for CO_2 storage because of their favourable characteristics. In this research, the Finite Element Method (FEM, ANSYS Student 2019 R2) was used to compute the optimum salt cavern shape that can be excavated by deep solution mining. Investigated shapes were spherical, teardrop, pear, bulb, and cylindrical shape. All of the caverns are designed to have a volume of ~520,000 m^3, allowing for the storage of ~0.4 million tons of CO_2 in its supercritical fluid state. The safety factor value and volume change were used as criteria to define which cavern shape is most suitable for CO_2 storage. The area around drill hole K-89 in Ban Nong Plue, Borabue district, Maha Sarakham province, northeast Thailand, was chosen as location for CO_2 storage because the sources of CO_2 are in immediate vicinity of potential sinks. Input parameters used in the modeling process are cavern geometry, material properties (lithologies), and creep parameters of rock salt. The creep constitutive model used in this case study is the Norton creep power law which defines the steady-state stage of creep. The modeling steps follow the operation stages of CO_2 storage, from the solution mining to the 500-year time span after cavern closure. The results indicate that the difference in the width in the upper part of the cavern (1/3 of the cavern height) influences the volume change. The smaller the width the lower the volume change, all caverns having the same height with the exception of the cylindrical cavern. Additionally, the results show that all the designed shapes have a safety factor value greater than 1, making them technically viable for being used as a Carbon Dioxide Storage in northeast Thailand. The optimum shape for storing CO_2 in its supercritical fluid state, maximizing the cavern stability, is the teardrop shape with a safety factor value of 6.36, also exhibiting the lowest volume shrinkage (0.018%) of all investigated shapes.

ACKNOWLEDGEMENTS

TABLE OF CONTENTS

Page

จุฬาลงกรณ์มหาวิทยาลัย

CHULALONGKORN UNIVERSITY

LIST OF TABLES

LIST OF FIGURES

LIST OF SYMBOLS AND ABBREVIATIONS

Symbols

E	Young's modulus
σ	Stress
ε	Strain
ρ	Density
m	Mass
V	Volume
ν	Poisson's ratio
$\varepsilon_{lateral}$	Lateral strain
ε_{axial}	Axial strain
Δl	Change in length
l_0	Initial length
Δd	Change in diameter
d_0	Initial diameter
$\dot{\varepsilon}_{cr}$	Steady state creep strain rate
A	Pre-exponential constant
n	Stress exponent
Q	Activation energy
R	Gas constant
T	Temperature
σ_e	Von Mises stress
σ_1	Major principal stress
σ_2	Intermediate principal stress
σ_3	Minor principal stress

SF	Safety factor
UCS	Uniaxial compressive strength
Lat.	Latitude
Long.	Longitude

Units

$^\circ$C	Degree Celsius
cm	Centimeter
GPa	Gigapascal
J	Joule
K	Kelvin
kg	Kilogram
km	Kilometer
km^2	Square kilometer
m	Meter
m^2	Square meter
m^3	Cubic meter
mol	Mole
MPa	Megapascal
Mton	Million tons
Pa	Pascal
s	Second

CHAPTER 1

INTRODUCTION

1.1 General introduction

Nowadays, huge amounts of anthropogenic carbon dioxide (CO_2) are being emitted, especially from industries using or exploring fossil fuels; for example, coal fired power plants or the oil and gas industry. CO_2 is one of the greenhouse gases which cause global warming. Moreover, CO_2 also causes ocean acidification by reacting with water forming carbonic acid (H_2CO_3). The acid affects sea creatures and corrodes cement or metal structures. Carbon capture and storage (CCS) is one of the methods to reduce the amount of CO_2 emissions emitted into the atmosphere. CO_2 will be captured at the sources, then transported via pipelines or trucks, and subsequently stored at the storage area. Most of the CO_2 will be stored in geological formations, for example, depleted oil and gas reservoirs, un-mineable coal seams, or deep saline formation (Bachu, 2003; Bachu & Rothenburg, 2003a; Dusseault, Bachu, & Rothenburg, 2004; Dusseault., Bachu., & Davidson., 2001; Wang et al., 2013).

Recently, researchers conducted research to find an alternative geological storage for CO_2, salt caverns being one of the alternative choices. Salt caverns are cavities left from the finished process of solution mining or a salt mine. There are many reasons for choosing salt caverns to store CO_2, for example, the crystalline structure of the rock salt with negligible porosity. The permeability of rock salt is very low with values around 10^{-21} - 10^{-24} m^2 (Wang et al., 2013). Therefore, rock salt can act as a seal, trapping most fluids and gases. Another advantage of rock salt is its self-healing capability. Fractures and cracks or damage due to changes of the gas pressure inside the caverns may heal by themselves over time. Furthermore, rock salt being a soluble material, the construction of salt caverns can be controlled, especially the shape. Additionally, salt layers are easily found in almost every part of the world where evaporite deposits formed. There are two important salt basins located in the Northeastern part of Thailand, the Khorat and Sakon Nakhon basin. Salt

layers in these basins are part of the Maha Sarakham Formation. These are some of the advantages of using salt caverns as a CO_2 storage.

There are lots of good reasons for using salt caverns as a geological storage; however, there are also some challenges that have to be dealt with. The creep properties of the rock salt and the gas pressure are some of the factors which can lead to the deformation of the structure, for example, volume change (decrease of the cavity's volume), ground subsidence above the cavern, or the collapse of the salt cavern (worst case) (Wang et al., 2013). Therefore, when designing the shape of the salt cavern it is of utmost importance to increase the safety factor and mitigate potential negative effects. Many factors are involved in the design, such as the material properties of rock salt and gas filling, geological structures of that area, etc.

In this research, the Finite Element Method (FEM) is used to evaluate the stability such as safety factor and percent volume change of the designed salt cavern for CO_2 storage in the Maha Sarakham Formation. Geomechanical properties of the rock salt such as uniaxial compressive strength (UCS), young's modulus, poisson's ratio, etc., the properties of the CO_2, and the structural inventory of the salt basin are considered in the salt cavern design in order to maintain the long-term stability of the CO_2 storage facility within the Maha Sarakham Formation.

Moreover, all parameters are related to each other. There are four main problems that need to be addressed;

-The shape and dimension of the salt cavern

Shape and dimension are key factors in terms of stability of the CO_2 storage. A different shape has a different ability to ensure stability, reduce volume change, etc.; likewise, differences in dimension and orientation also influence the salt cavern stability even though the shape is the same. As a result, the shape and dimension are difficult problems in designing the salt caverns.

-Quantity of the CO_2 to be filled in the salt cavern

The quantity of the CO_2 emissions, especially from the power plant and oil and gas industry, needs to be known for designing the salt cavern size. The volume of the cavern (total volume of the caverns) should be adequate to store the emitted CO_2.

-The aggregate state of the CO_2

The aggregate state of the CO_2 in which it is to be stored in the salt cavern is one of the important factors that needs to be addressed. Depending on the aggregate state, gas or supercritical fluid, different pressures will be acting on the wall of the cavern(s). The design will be adapted to suit the properties of the CO_2 inside the cavern. In addition, the temperature of the CO_2 can also affect the rock salt properties, e.g. creep behavior.

-The location to develop the CO_2 storage

Different locations may have different geological structures which may lead to different material properties such as strength, etc. In addition, the temperature and pressure increase with increasing depth (geothermal gradient and lithostatic pressure). An increase in temperature and pressure can affect the salt cavern stability, but the deeper salt layers of the Maha Sarakham Formation tend to be thicker than the shallower layers. Therefore, when choosing the location to construct the CO_2 storage, especially the depth should be considered.

1.2 Objectives

- To find the optimum shape of the salt cavern for CO_2 storage in the Maha Sarakham Formation, Northeast Thailand.
- Evaluation of the long-term stability of the salt cavern.
- Identify possible locations for CO_2 storage in salt caverns in Northeast Thailand (tentative).

1.3 Scope of research

The scope of this research will cover;

- Designing the shape of the salt cavern that can be developed by the deep solution mining method (depth more than 800m).
- Optimizing the salt cavern shape by using the input parameters based on material properties and geological structures.

- Evaluating the long-term stability of the salt cavern with focus on the transient volume change of the salt cavern.

- Screening possible locations for CO_2 storage in the Maha Sarakham Formation, Northeast Thailand.

1.4 Expected benefits from research

- Establish salt caverns in the Maha Sarakham Formation as an alternative for CO_2 storage in Thailand.

- The amount of CO_2 emissions from power plants released into the atmosphere would be reduced if CO_2 can be captured and stored in the salt caverns.

1.5 Order of presentation

The author has divided the thesis into 6 chapters as follow;

Chapter 1 Introduction: General introduction, research objectives, scope of this research, expected benefits and outline of this study.

Chapter 2 Background and literature reviews: Overview in CO_2 emissions in Thailand, geology of Northeast Thailand, solution mining, and literature reviews.

Chapter 3 Geomechanical modeling: Modeling method, model geometry, material properties used in the geomechanical modeling, and construction and operation stages of the salt cavern (modeling steps)

Chapter 4 Results and discussions: Results and discussion of the modeling in each shape.

Chapter 5 Conclusion: Conclusion and recommendation.

CHAPTER 2

BACKGROUND AND LITERATURE REVIEW

2.1 Background

2.1.1 CO_2 emissions in Thailand

CO_2 is a greenhouse gas which causes an increase of Earth's temperature (Global warming). Although there is a consensus about the impact of anthropogenic CO_2 on the global climate within the scientific community it is still denied by some fringe groups. The fossil fuel industry; oil, gas and coal, has been pressured by society for emitting huge amounts of CO_2 into the atmosphere. Therefore, the industry chose to take responsibility for emitting the CO_2. One of the possible choices is CO_2 capture and storage (CCS) (Dusseault et al., 2004).

The statistics of the CO_2 emission in Thailand in 2018 as shown in figure1; overall emission of CO_2 in Thailand in the year 2018, Thailand emitted 260.48 million tons of CO_2. The electric power generation sector emitted the highest amount of CO_2 with 94.32 million tons (36% of CO_2 emission), followed by the industry sector (31%), the transportation sector (26%) and others (7%). Figure 2 shows the graph of CO_2 emission in Thailand from year 1989 to 2018 which slightly increased every year (Energy Policy and Planning Office, 2018).

In Northeast Thailand CO_2 emissions originate from several smaller biomass power plants and a fossil fuel power plant (natural gas) (Figure 3). The biomass power plants emit 0.456 million tons of CO_2 per year. The natural gas power plant, which satisfies most of the electricity needs in Northeast Thailand, emits 2 million tons of CO_2 per year, making it the main contributor to greenhouse gas emissions in the region (Choomkong, Sirikunpitak, Darnsawasdi, & Yordkayhun, 2017).
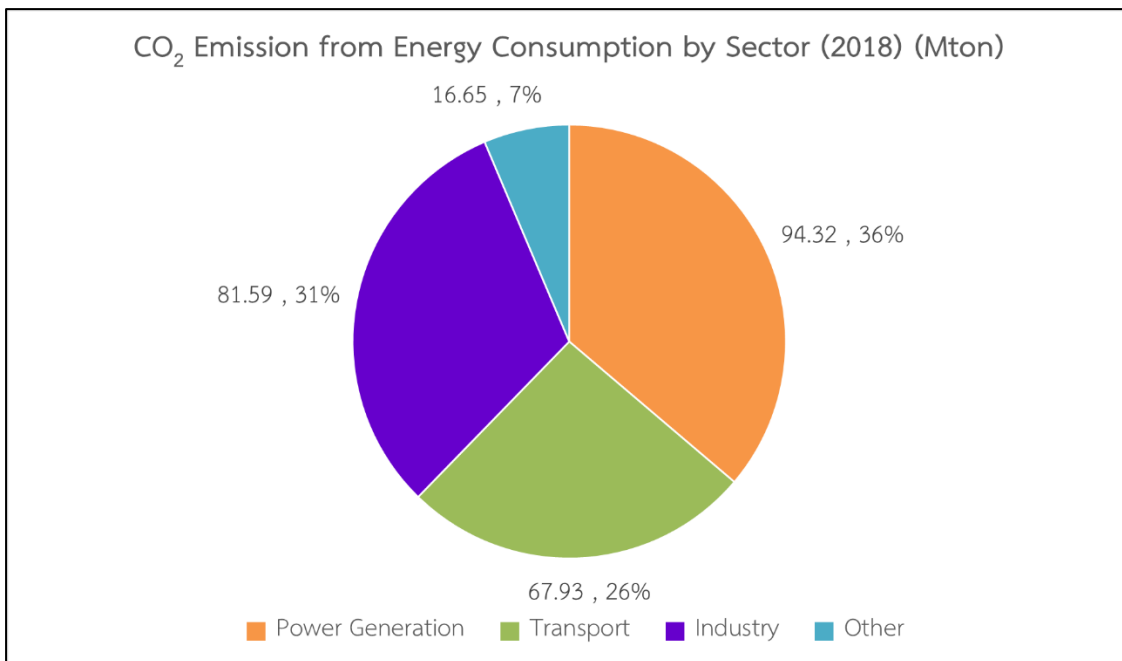
Figure 1: CO_2 emission from Energy Consumption by Sector (modified from Energy Policy and Planning Office, 2018)
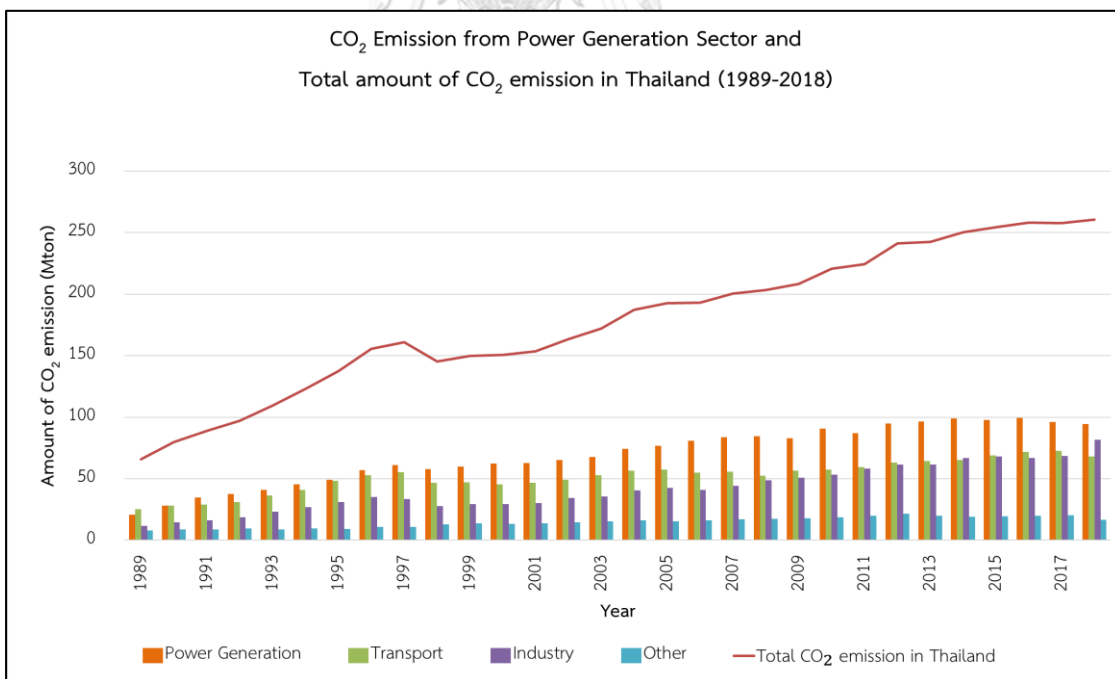
Figure 2: CO_2 Emission from Power Generation Sector and Total amount of CO_2 emission in Thailand (1989-2018) (modified from Energy Policy and Planning Office, 2018)

2.1.2 Geology of Northeast Thailand

The Northeastern part of Thailand covers about one-third of the country. The important evaporite deposits in this region are within the Khorat and Sakon Nakhon basin. The two basins are separated by the Phu Phan anticline as shown in figure 3. The Maha Sarakham Formation is present in both the Khorat and Sakon Nakhon basin (El Tabakh, Utha-Aroon, & Schreiber, 1999; Utha-Aroon, 1993).
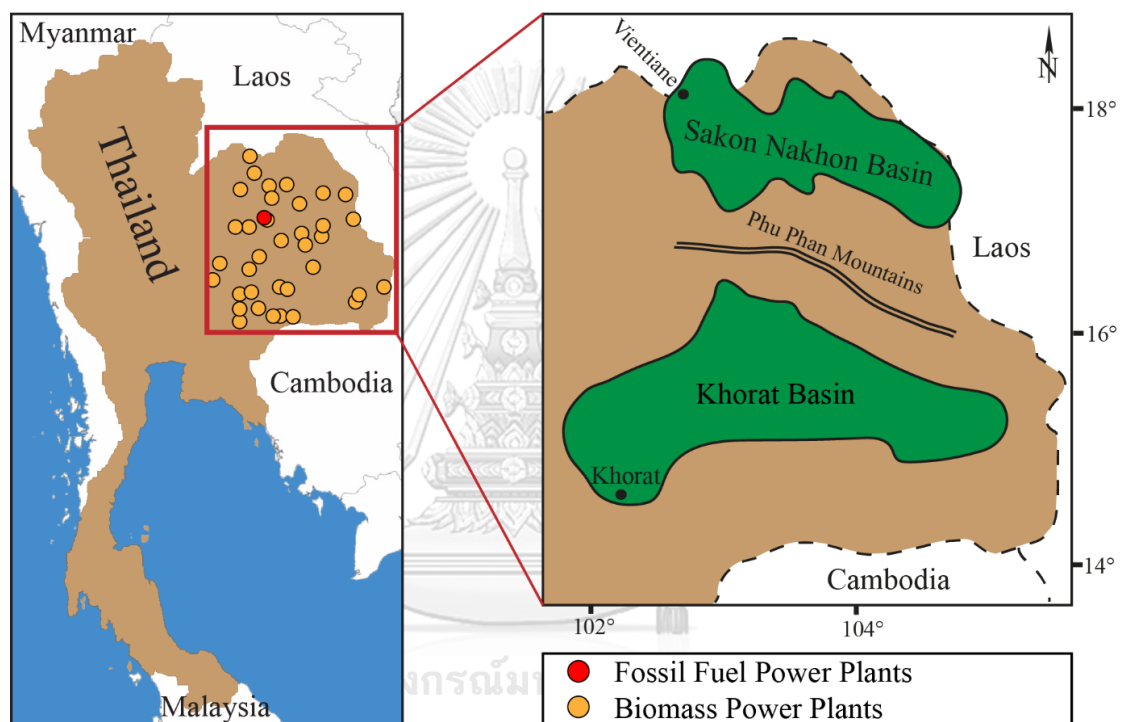
Figure 3 : Location of CO$_2$ emission sources from fossil fuel and biomass power plants in Sakon Nakhon basin and Khorat basin, Northeast Thailand (modified from El Tabakh et al., 1999; Choomkong et al., 2017)

The Maha Sarakham Formation is an evaporite deposit of Cretaceous to early Tertiary age. The formation has an average thickness of 250 m, reaching up to 1.1 km in the thickest parts. The formation can be divided into three main layers which are Upper member, Middle member and Lower member. Figure 4 shows the lithostratig-raphy of the Maha Sarakham Formation. The lower member, Halite L1 and Halite L2,

exhibits a thickness suitable for the excavation of a salt cavern to store CO_2 (El Tabakh et al., 1999).
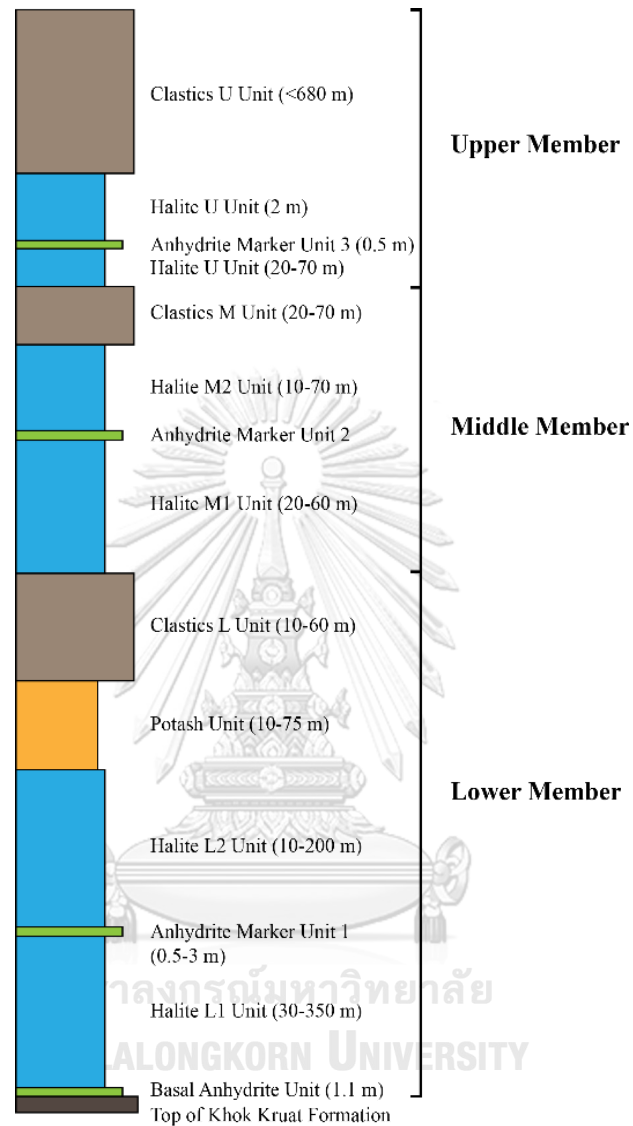
Figure 4: Lithostratigraphy of a complete sedimentary section of the Maha Sarakham Formation

2.2 Literature review

2.2.1 Solution mining inThailand

In Thailand, Pimai Salt Co.,Ltd. is the only mining company in Thailand that used solution mining method by dissolving rock salt to produce brine product. Pimai

Salt Co.,Ltd. located in Pimai district in Nakhon Ratchasima province. Salt caverns are mined by using direct circulation method with an annual production of over 1 million tons which used oil as a blanket material. The caverns are mined in Lower Salt member of Maha Sarakham Formation at 200 to 280 meters depths. The cavern shape is a modified cylindrical shape with cavern volume of 600,000 m^3. The cavern diameter and height are 80 and 45m respectively. The spacing between the center of the caverns is 120 m (Groenefeld, Yoshida, Koder, & Bunpapong, 1993).

Vattanasak (2006) researched in salt reserve estimation for solution mining in the Khorat basin by designing the salt cavern in several depths in the Lower Salt Member of the Maha Sarakham Formation. The suggested shape for the cavern is a sphere with a diameter of 60m. FEM simulations have shown that the cavern will retain its stability for at least the next 50 years. The ground subsidence for the shallowest cavern (200 m depth) and deepest cavern (400 m depth) is 2.92 cm and 6.45 cm respectively. With these magnitudes of the subsidence, it is considered to have no harmful effect on the structures and on the surrounding environment.

2.2.2 Salt cavern for natural gas storage and CO_2 storage

Nowadays, salt cavern is used as a storage facility; for example, salt cavern for natural gas storage. Natural gas is injected into the cavern when the electrical power demand is low, and it will be discharged to generate the electricity when the demand is high. Therefore, the natural gas storage cavern is operated under the cyclic load whereas the cavern for CO_2 storage is closed after the CO_2 injection. The CO_2 from power plants or the oil & gas industry. Besides storing CO_2 in the salt cavern, CO_2 can be stored in geological formations such as depleted oil and gas reservoirs, un-mineable coal seams, and deep saline aquifers. The reasons of using salt caverns are (i) the low permeability and crystalline structure of the rock salt, (ii) the wide distribution of salt basins, (iii) self-healing capability of the rock salt after the damage, (vi) rock salt is a soluble mineral, so shape and dimension can be controlled during the cavern construction (Dusseault et al., 2004; Shi & Durucan, 2005; Wang et al., 2013).

Many researchers have modeled salt caverns into different kinds of shape and dimension. Differences in shape and dimension cause a difference in stability of the salt caverns. The shape and dimension also depend on the material properties, location, geological structures, and the aggregate state of CO_2 in the cavern.

Mraz (1980) constructed many shapes of salt cavern models. The results show that the ellipsoid shape cavern can reduce its volume shrinkage and kept its stability better than among other shapes.

Dusseault et al. (2004) designed a salt cavern for storing CO_2 in supercritical fluid form in the Lotsberg salt, Canada. At 1.2 km depth, a sphere with a diameter of 100m is modeled in this research. There are two scenarios were modeled in this research. First one is the cavern is sealed after the CO_2 injection where the cavern pressure is at 50% of lithostatic pressure. Second scenario is pre-pressurized greater than the hydrostatic pressure of the brine before sealing the cavern. The result shows that the volume reduction of the cavern will be reduce by 10-15% if the cavern is pre-pressurized before the cavern closure. In addition, the internal pressure inside the cavern will reach 95% of the lithostatic pressure after 4,000 years of cavern closure. For ground subsidence result, the model shows that approximately of 5 mm of subsidence occurs at the ground surface.

A. Costa et al. (2011) studied on underground storage in deep and ultra- deep water offshore for natural gas and CO_2 storage under the cyclic load. The Santos basin which presents the Pre-salt reservoirs was chosen as a case study. Twelve cylindrical shaped caverns with 300 m height and 100 m span were used in the model where top of the cavern located at 2901 m depth from the water surface. The results show that during thirty-year period of operation, the caverns will be stable in by using the minimum pressure of 50% of the initial stress.

Wang et al. (2013) studied a new model to design dimension and shape of the salt cavern for gas storage under the cyclic operation by dividing the cavern into two parts; upper and lower part. The results of the research show that the minimum of the gas pressure specified the shape and dimension of the upper structure of the cavern. On the other hand, the maximum of the gas pressure specified the lower structure of the cavern.

Feunkajorn (2013) used creep parameters to simulate the creep deformation of CO_2 storage salt cavern by using Finite difference method. The creep parameters were tested by the uniaxial creep test to find the effect of low temperature on time-dependent deformation of rock salt in Maha Sarakham Formation. Constant temperatures which are 0°C and 30°C are applied to the test. The test took 21 days. Time-dependent deformation of rock salts described by exponential creep law. The cylindrical cavern as shown in figure 5 is designed by using the radius of 25 m located in 500 to 1000 m depth. The results show that the stress distribution of both temperatures is similar but the radial closure for the cavern under low temperature is 10% less than the cavern under room temperature.
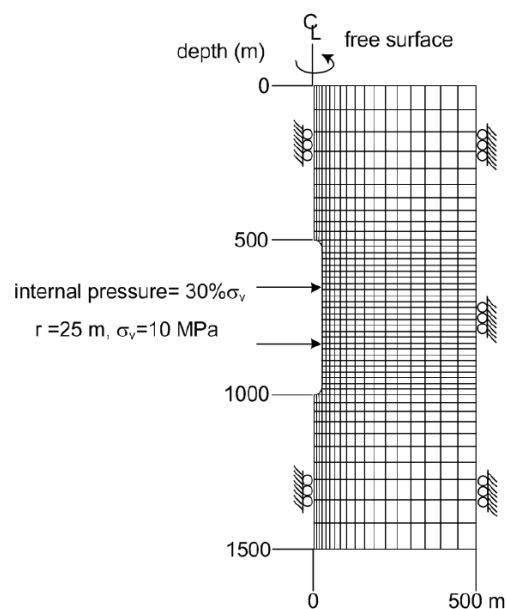
Figure 5: The diagram of designed salt cavern from FLAC4.0 (Feunkajorn, 2013)

P. Costa, Roehl, Costa, Amaral, and Poiate Jr (2014) studied underground salt caverns for brine production and natural gas storage. The salt cavern for natural gas storage is designed to be used under a maximum pressure during the low demand of electricity and minimum pressure in order to keep the cavern stable. In the model, the top of cylindrical cavern located at 1228 m depth. The dimension of the cylindrical cavern is 200 m height and 100 spans. The geometric volume of the cylindrical cavern is 1.2 million m³. The results from the numerical simulation show that volume

of natural gas at the maximum pressure is 281 million m^3 and volume of natural gas at the minimum pressure of 106 million m^3 which is potential to use as a gas storage.

Yang et al. (2015) studied on feasibility analysis of using abandoned salt cavern for underground gas storage (UGS) in Jiangsu province, China. The geomechanical numerical simulations is used to evaluate the abandoned salt cavern. There are two caverns which are pear shaped and cone shaped cavern were used in the simulation. Both shapes have the approximate volume of 100,00 m^3. The top of the cavern is located at approximate 900 m depth. The results show that the maximum volume shrinkage is less than 25% after 20 year of operation. Safety factors value is decreased with the operating time. The analysis results indicate that using of the abandoned salt cavern as a UGS is quite feasible and reliable where the first salt cavern gas storage facilities in China were completed. Gas was first injected into the cavern in 2007 to check the stability of the caverns after 6 years of operation. Measurement of cavern's volume shows that there is less change in cavern shape, and the volume shrinkage is less than 2%.

From reviewing the related literatures, it shows that the different in shapes of the salt cavern have an effect to the cavern stability and volume change of the cavern. However, the optimum shape for CO_2 storage cavern remains unclear. Therefore, geomechanical modeling of different salt cavern shapes for storing CO_2 in supercritical fluid form that can be conducted by deep solution mining will be the main purpose of this research. The geomechanical modeling process and all variables used in the models are explained in the next chapters.

CHAPTER 3

THEORETICAL BACKGROUND

For the geomechanical modeling, the basic knowledge of solution mining processes and techniques to control the shape of the cavern are required to model the salt cavern. Moreover, the basic theory of Finite Element method which is the numerical method is needed. Finite Element method is used as an analysis tool to compute the stability of the salt cavern in this research. All parameters such as input, and output parameters involved in the analysis are defined in this chapter.

3.1 Solution mining

Besides conventional underground mining methods, e.g. room and pillar, solution mining is commonly used for exploiting evaporite minerals, such as rock salt or potash. Based on history records, solution mining has been used for at least 8,000 years (Jeremic, 1994).

Solution mining is a method exploiting the favorable characteristic of rock salt which is the solubility of salt in water. The fundamental process of solution mining is developing a wellbore to the salt layers, injecting water to dissolve salt minerals creating a saturated brine and discharging the brine from the salt cavern. The advantage of solution mining is the exploitation can be done without removing the overburden lying on top of the orebody. Moreover, mine development period of the solution mining takes less time compared to other underground mining methods where access facilities, such as shaft and incline need to be developed first in order to exploit the ore. Consequently, the capital cost of solution mining is lower than the conventional underground mining method. The disadvantage of the solution mining method is the limitation of minerals that can be exploited. The minerals should be soluble. The cavern stability and ground subsidence need to be managed with the utmost care by designing and controlling shapes and sizes of the cavern (Allen, Doherty, & Thoms, 1982; Jeremic, 1994).

3.1.1 Solution mining process

As above-mentioned, after developing a wellbore, water will be injected to dissolve rock salt. A salt cavern is formed in this stage. The common ways to control the shape of the cavern are use of a blanket material and control of the circulation system in the cavern.

Blanket material is a fluid-like material that injects into the cavern in order to protect the unwanted dissolve area as shown in figure 6, for example the area around the cemented casing where stability is crucial. The blanket is also used to limit the dissolving area at the roof of the cavern. Therefore, the blanket is required to have a lower density than water and not be able to dissolve the salt.
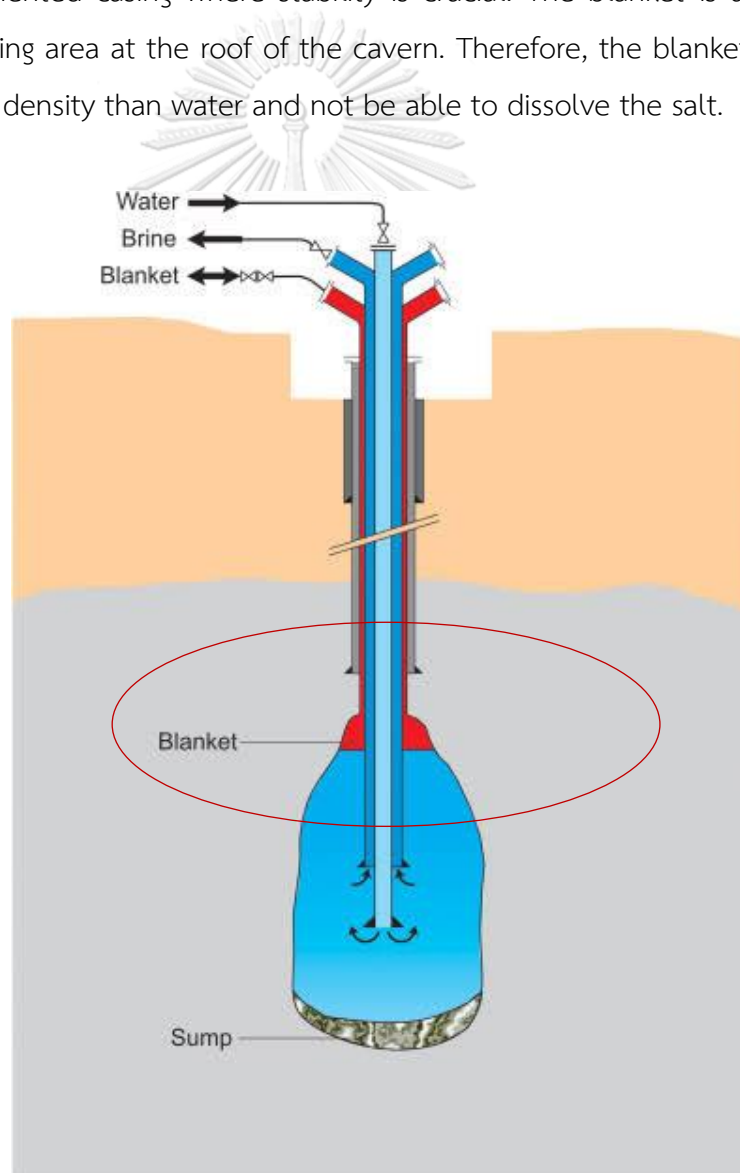
Figure 6: Using of the blanket in the direct solution mining (K-UTEC- Sondershausen)

3.1.2 Solution mining techniques: Circulation method

The circulation method of solution mining also influences the shape of the cavern. Two circulation systems have been generally used in the solution mining which are (Allen et al., 1982; Jeremic, 1994);

- **Direct circulation method:** water is injected at the bottom part of the cavern and the brine is discharged near the area at the blanket casing as shown in figure 7. Using this method, the shape of the cavern will be enlarged at the bottom and narrowed at the upperpart of the cavern. For example, teardrop, pear, spherical shape are the results from using the direct circulation method. Cylindrical shape also can be excavated by the direct circulation method, but the water injection tube will be moved along the height of the cylindrical cavern.
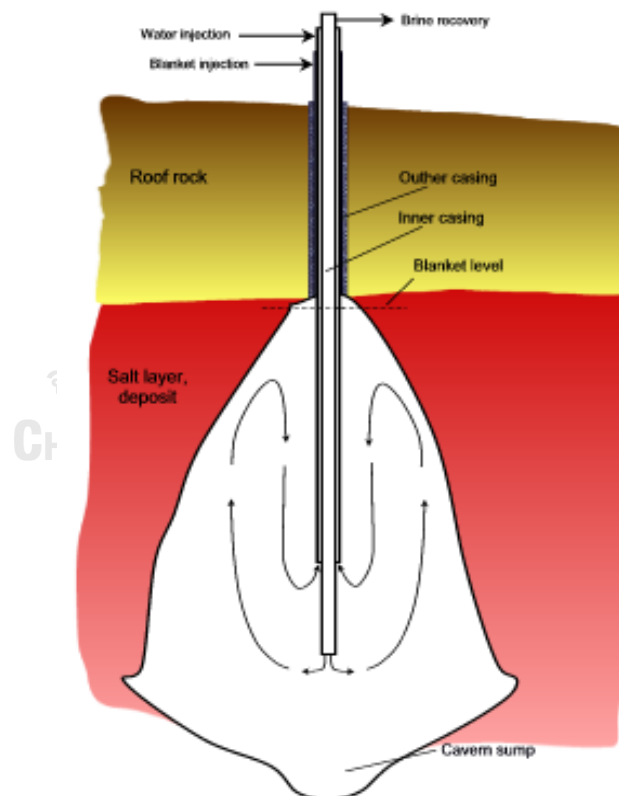
Figure 7: Solution mining by using direct circulation method (K-UTEC-Sondershausen)

- **Indirect method:** or reverse circulation method, uses the same set-up as the direct circulation method, but the flow of the injected water is reversed as shown in figure 8. The water is injected in the upper part of the cavern, so, the system can be called a top injection method. The brine will be discharged from the bottom part of the cavern. This method is used to develop the upperpart-enlarged cavern such as bulb shape.
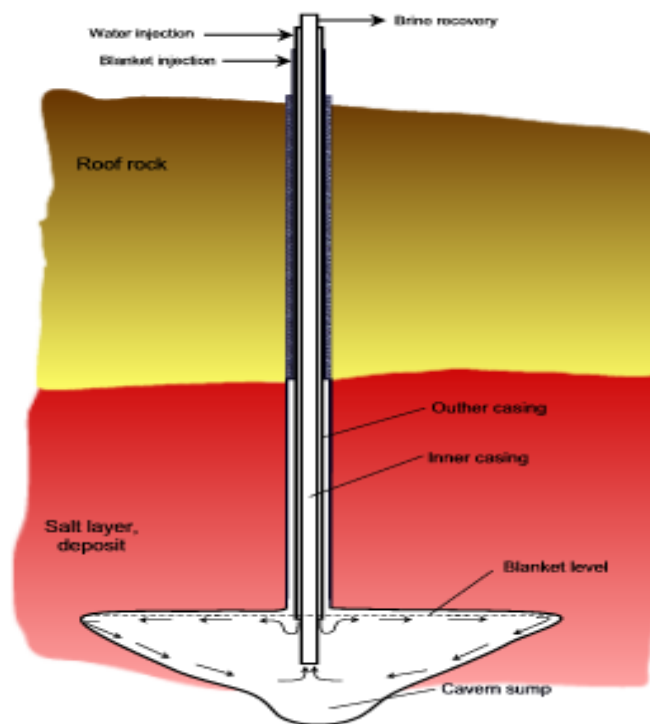
Figure 8: Solution mining by using indirect circulation method (K-UTEC-Sondershausen)

All above mentioned methods are circulation type solution mining methods. Solution mining can also be categorized by the number of wells used to develop a cavern, which are single-well method, and two-well method.

The Single well method uses only a single large wellbore. The injection tube and brine discharge tube will be located in the same borehole. In contrast, for the two-well method, two wells are drilled in order to separate the injection well and

the brine discharge well. The connection of the cavern is done by using the high-pressure water injection to cause the fracturing between two wells as shown in figure 9. From using the two-well method an ellipse shaped cavern is formed. Due to the large spans of the cavern compared to other shapes, the problem of roof collapse is a major concern. Therefore, this type of excavation is limited to the depth not exceeding 500m (Jeremic, 1994).
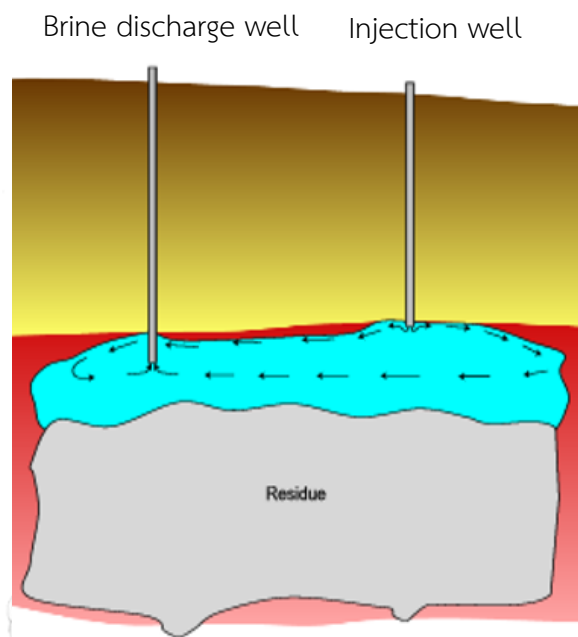
Figure 9: Solution mining by using two-well method (K-UTEC- Sondershausen)

3.2 Finite Element Method

The Finite Element Method (FEM) is a numerical method for solving complicated problems within mathematics or engineering such as a complicated geometry. FEM is useful in many applications; for example, heat transfer, structural/ stress analysis, etc. The principles of FEM consist of model discretization, selection of constitutive equation for matrix formulation, solving the unknown as a nodal solution. Finite Element Method can easily be compared as the Hooke's law of a spring. Equation 1 shows the Hooke's law relationship of the spring (Boonyatee; Madenci & Guven, 2015; Mehta & Joshi, 2016).

$$F = ku \qquad (1)$$

Where; F is a force;

              k is a stiffness of spring;

              u is a displacement of a spring

When force (F) is applied to the spring, the displacement (u) occurs. The magnitude of the displacement will be different because of the different in stiffness of the spring k.

The Finite Element Method basic matrix formulation is shown in equation 2.

$$[F] = [K][u] \qquad\qquad (2)$$

Where; $[F]$ is a boundary condition;

              $[K]$ is a material property;

              $[u]$ is a nodal solution

In Finite Element Method, the model is divided into elements where nodes connect each of elements together in this step is called discretization the domain or meshing. Constitutive equation is selected to define stress-strain relationship of the material. Then, the properties of materials are defined in order to build the stiffness matrix of each element or $k_{element}$. After building the $k_{element}$, a global stiffness matrix ($[K]$) is defined by assemble all $k_{element}$ from the local coordinates to global coordinates. Then, the boundary conditions such as force, applied stress, etc. are set into the $[F]$ matrix in order to solve the primary unknown or nodal solution which is $[u]$ matrix which lead to solve the secondary unknow. In this research, the primary unknown is displacement, where the secondary unknown are stress, strain, etc.

To summarize the basic concept of the Finite Element Method, the process is followed by these steps;

1) Discretization the domain (Meshing)

2) Selection of the Constitutive equation

3) Building element stiffness matrix ($k_{element}$)

4) Assembly global stiffness matrix (corporate $k_{element}$ into $[K]$)

5) Introducing the boundary condition ($[F]$)

6) Solving the primary unknown: nodal solution $[u]$

7) Solving the secondary unknown

3.3 Input parameters

In the modeling, input parameters consist of two main variables which are geological variables and geometrical variables as explain below;

3.3.1 Geological variables

For geological variables using in the model are the variables involve with the material properties. In geomechanical modeling, Young's modulus, Poisson's ratio, uniaxial compressive strength, density, and creep parameters are used.

Figure 10 illustrates the relationship of the stress and strain of the material which is the result of uniaxial compressive strength test.
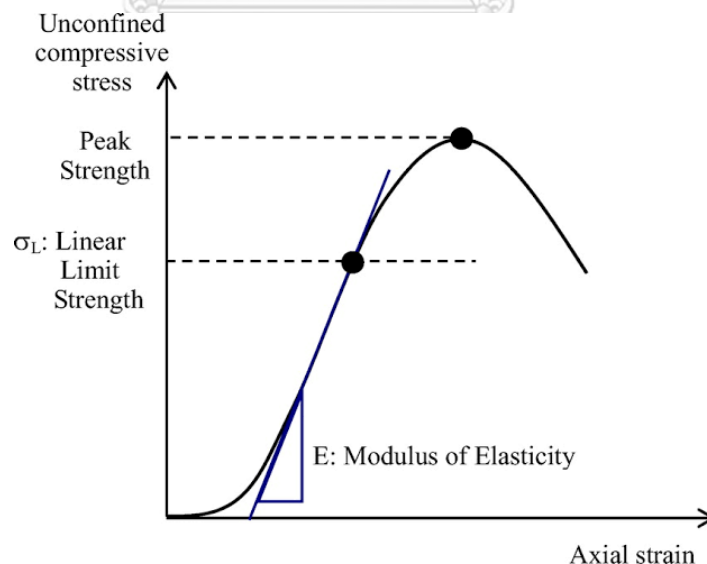
Figure 10: Stress-strain relationship (Park, 2010)

3.3.1.1 Young's modulus

From figure 10 shows that Young's modulus or Modulus of elasticity (E) is the range which the stress is proportional to the strain. It means that the material returns to its original position when the stress is removed (Hudson & Harrison, 2000). The equation of Young's modulus is shown in equation 3;

$$E = \frac{\sigma}{\varepsilon}$$

(3)

Where; E is a Young's modulus;

σ is a stress;

ε is a strain

3.3.1.2 Uniaxial compressive strength (UCS)

Uniaxial compressive strength or peak strength in figure 10 is the maximum axial compressive strength that the material can endure before fracture (Hudson & Harrison, 2000).

3.3.1.3 Poisson's ratio

Poisson's ratio is the material property that shows the relationship between the lateral strain and axial strain when the load is applied on the sample as shown in figure 11 (Hudson & Harrison, 2000). The equation of Poisson's ratio is shown in equation 4;

$$\varepsilon_{lateral} = \frac{|d_0 - d|}{d_0}$$

$$\varepsilon_{axial} = \frac{|l_0 - l|}{l_0}$$
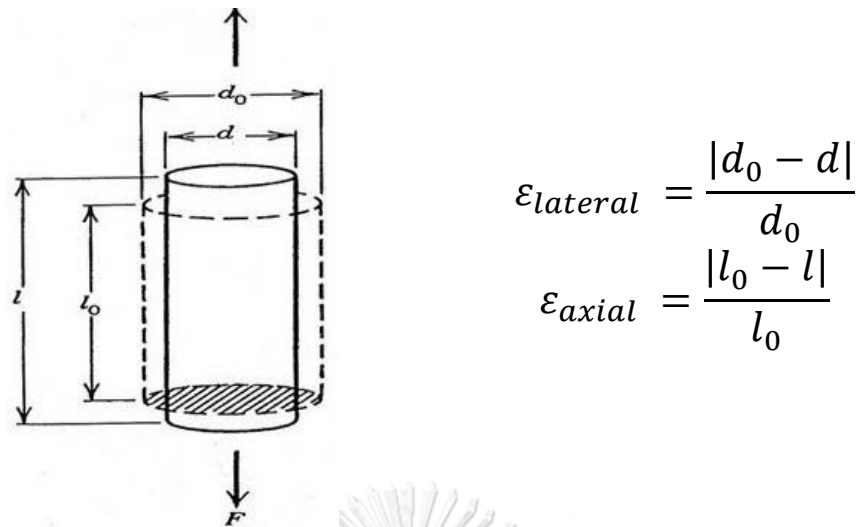
Figure 11: Poisson ratio of the material (Divedi, 2017)

$$\nu = -\frac{\varepsilon_{lateral}}{\varepsilon_{axial}} \qquad\qquad (4)$$

Where; ν is a Poisson's ratio;

$-\varepsilon_{lateral}$ is a lateral strain;

$-\varepsilon_{axial}$ is an axial strain

3.3.1.4 Density

Density is a mass per unit volume of the material (Hudson & Harrison, 2000). The relationship is shown in equation 5;

$$\rho = \frac{m}{V} \qquad\qquad (5)$$

Where; ρ is a density;

m is a mass;

V is a volume

3.3.1.5 Choice of a Creep Law

Salt exhibits viscoplastic behavior under differential stress. The temperature as well as the difference between the stress and the pressure within the cavern are used to predict the creep rate. A pressure increase in the cavern leads to a diminishment of this difference. Therefore, the creep rate slows and a stress state reflecting the stress field prior to the construction of the cavern (virgin stress) is approached asymptotically.

In our study, the salt mass is subjected to a relatively small range of temperature and differential stress. Consequently, a full constitutive model for the behavior of salt over a wide range of temperature and shear stress is not necessary (Carter, Horseman, Russell, & Handin, 1993). For our salt cavern models we focus on secondary or steady state creep acting over very long-time spans as shown in figure 12.
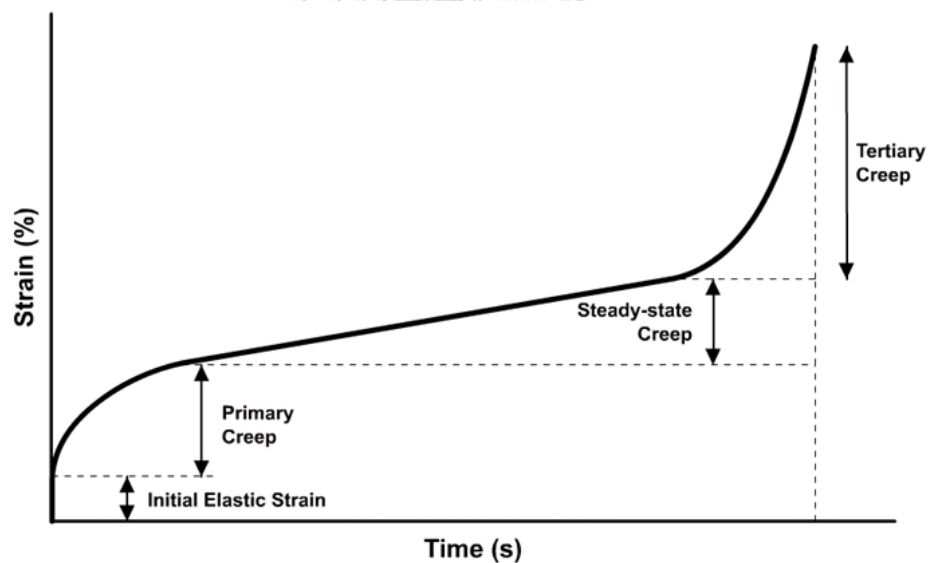
Figure 12: The creep curve: primary, steady- state, and tertiary creep stages (Spaceflight.esa.int., 2019)

The Norton Creep Power Law as shown in equation 6 was applied in our simulations.

$$\dot{\varepsilon}_{cr} = A\sigma^n \exp\left(\frac{-Q}{RT}\right) \qquad (6)$$

Where; $\dot{\varepsilon}_{cr}$ is a steady state creep strain rate;

A is a constant parameter;

σ is a stress;

n is a stress exponent;

Q is an activation energy;

R is a gas constant;

T is a temperature

3.3.2 Geometrical variables

For geometrical variables using in the model are the variables involve with the geometry of the caverns. In this research, the technical terms that define parts of the cavern are shown in figure 13. The cavern is divided into three parts which are upper part, center and lower part. Where roof means the upper part of the cavern, floor means the lower part of the cavern, and wall means the side of the cavern. For geomechanical modeling, salt caverns are designed into five different shapes which are spherical, bulb, teardrop, pear, and cylinder as shown in figure 14. All shapes are designed to have an approximate volume of 520,000 m³. The most important thing for designing shape of the salt cavern is that the shape should be able to develop by the deep solution mining method (depth more than 800m), either direct or indirect circulation. The difference in shape of the salt caverns is influenced by controlling the water injection and the blanket.
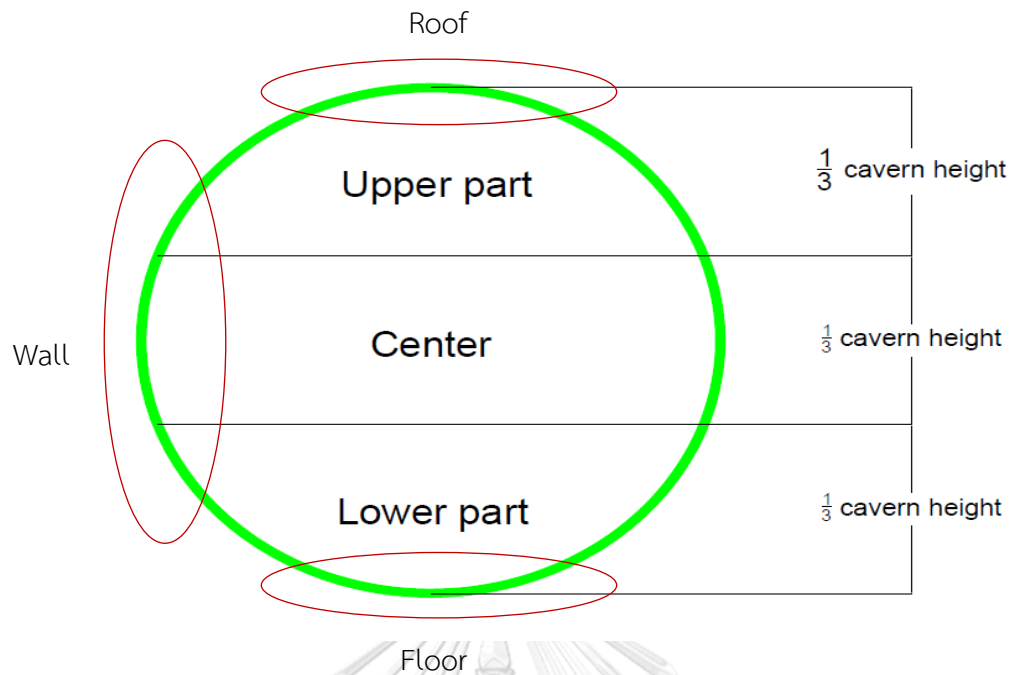
Figure 13: Terminology of the cavern parts used in this research

The techniques of circulation to conduct the different shapes cavern are mentioned as follow;

3.3.2.1 Spherical shape

For the spherical-shaped caverns, direct circulation will be used. But in reality, a perfect spherical cavern is difficult to mine by using solution mining.

3.3.2.2 Bulb shape

For the bulb- shaped cavern, indirect circulation method will be used to develop the cavern which favors to have the upper part expansion. For dissolving the lower part of the cavern, direct circulation technique can be applied.

3.3.2.3 Teardrop shape

For teardrop shaped caverns, direct circulation will be used in order to make the lower expansion of the cavern. Indirect circulation technique can be applied in order to dissolve the upper part of the cavern.

3.3.2.4 Pear shape

For the pear-shaped cavern, a mixed method, between direct and indirect circulation, is used. Where indirect circulation method is used in the cavern development phase and followed by the direct circulation method in the production phase.

3.3.2.5 Cylindrical shape

For the cylindrical shaped cavern, the direct circulation method will be used. The cavern will be excavated by injecting the water at the bottom of the cavern first, then the injection tube will be moved upward following the designed height in order to form the cylinder-shaped cavern.

Spherical shape   Bulb shape

Teardrop shape   Pear shape

Cylinder shape
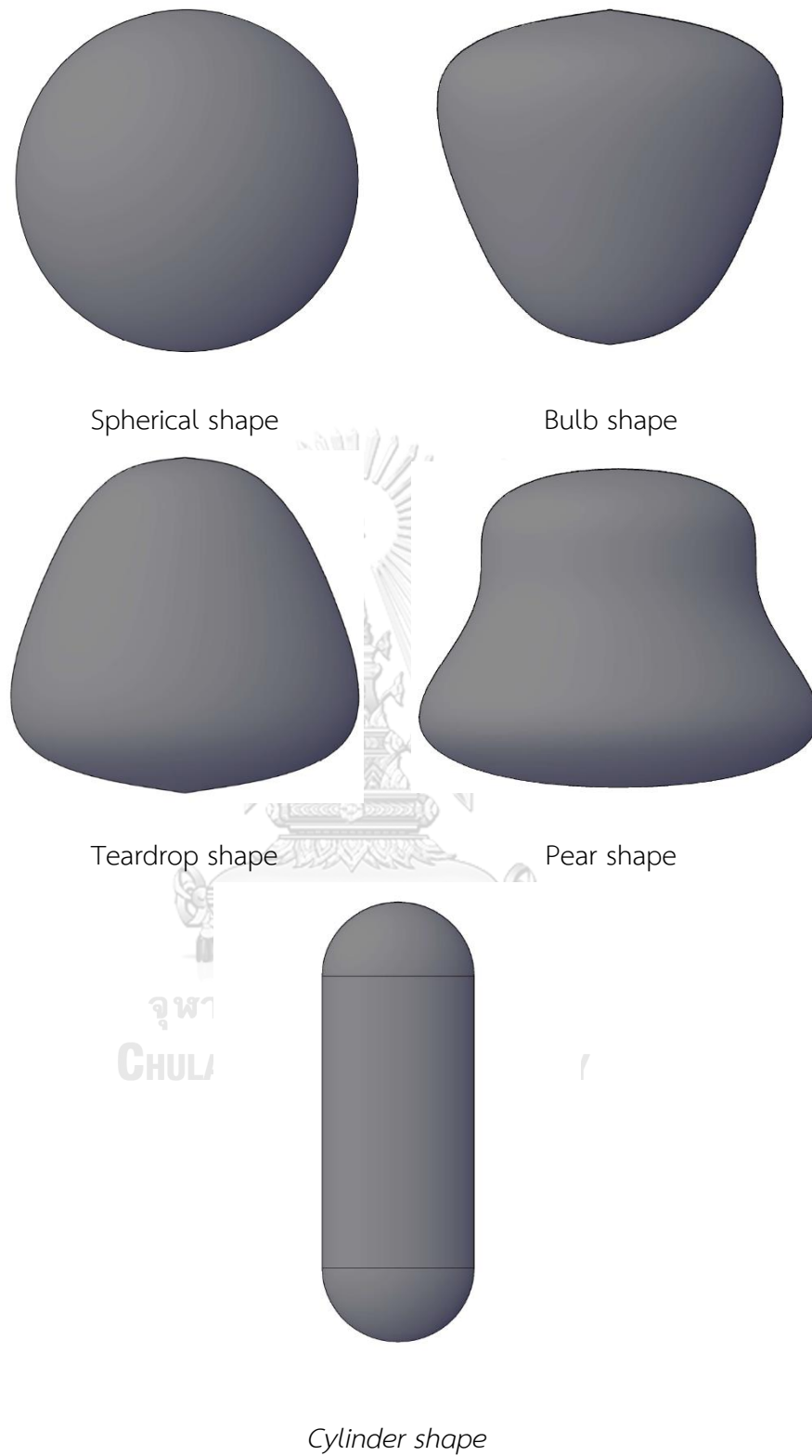
Figure 14: The designed shape cavern used in modeling

3.4 Output parameters

After the nodal solutions are solved, the results are used to compute the secondary unknowns. In this research, Von Mises stress, safety factor, volume change, and ground subsidence will be obtained as they are used as criteria to define which salt cavern shape is the optimum shape for storing CO_2 in supercritical state.

3.4.1 Von Mises stress

Von Mises stress or equivalent stress is a stress that represents the three principal stresses (σ_1, σ_2 and σ_3) in a single positive stress (Kohnhe, 2013). Figure 15 illustrates the principal stress components on cubic. Von Mises stress can be computed by using equation 7.
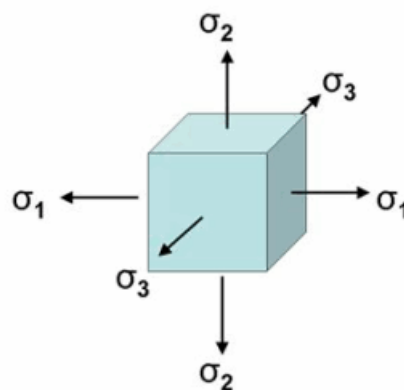
Three Principal Stresses σ1, σ2, σ3

Figure 15: Diagram of principal stress components (Value design Consulting, 2019)

$$\sigma_e = \left(\frac{1}{2}[(\sigma_1 - \sigma_2)^2 + (\sigma_2 - \sigma_3)^2 + (\sigma_3 - \sigma_1)^2]\right)^{\frac{1}{2}} \quad (7)$$

Where;　　　　σ_e　　　　is a Von Mises stress;

　　　　　　　σ_1　　　　is a major principal stress;

　　　　　　　σ_2　　　　is an intermediate principal stress;

　　　　　　　σ_3　　　　is a minor principal stress

3.4.2 Safety factor

Safety factor is a value use to refer that the structure is safe or not. If safety factor is more than one, it means that the structure is safe. In contrast, if the safety factor is less than one, it means that the designed structure is not viable to use (Kohnhe, 2013). In this research, Safety factor is calculated by using equation 8.

$$Safety\ factor\ =\ \frac{Uniaxial\ compressive\ strength}{Von\ Mises\ stress} \qquad (8)$$

3.4.3 Volume change

In this modeling, volume change is computed by exporting the coordinates of nodes at the cavern boundary and nodal displacement to find the coordinate after the operation, then imported to AutoCAD to find the volume of the caverns.

3.4.4 Ground subsidence

Ground subsidence in this modeling is the maximum magnitude of the displacement at the top surface of the model in each operation stage.

CHAPTER 4

GEOMECHANICAL MODELING

4.1 Modeling method

In this research, the Finite Element Method (FEM, ANSYS Student 2019 R2) is used to compute the salt cavern stability. The process will be divided into three steps: preprocessing, processing and postprocessing as shown in figure 16.
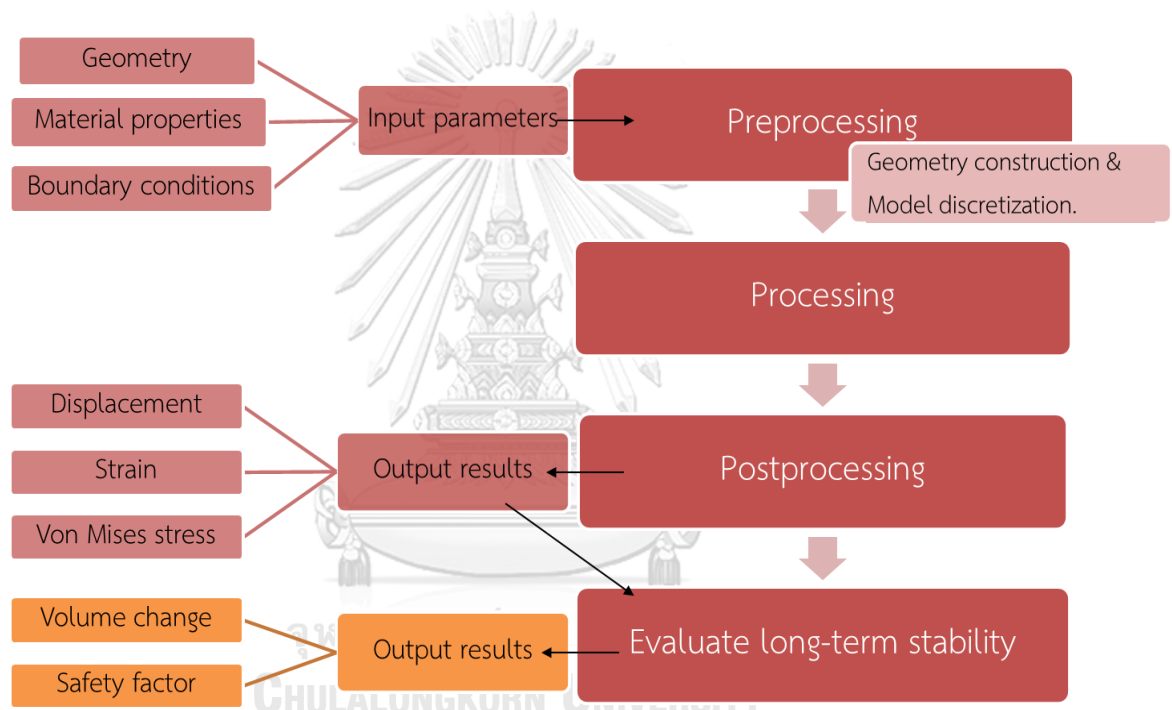
Figure 16: Flowchart of the FEM process: preprocessing, processing, and post processing

Preprocessing involves geometry, material properties and meshing (PLANE183: quadratic, 8 nodes, 2D elements, as shown in figure 17. Solutions for the model are obtained during the processing step which includes defining boundary conditions (forces or displacements) and the type of analysis (static vs. transient). The solution stage has been divided into four substages which will be mentioned in operation stage of salt cavern for CO_2 storage in further section. The results (stresses, displace-

ments, safety factor, volume decrease, etc.) obtained during processing can be viewed in the postprocessing step.
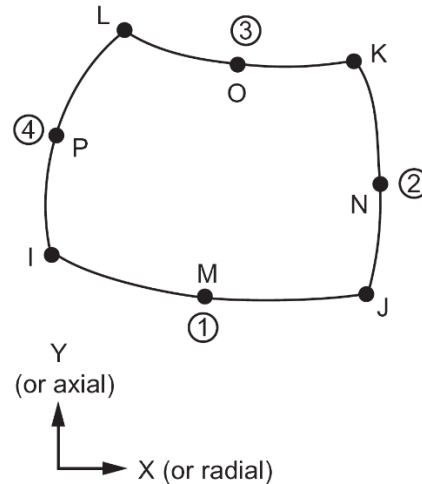
Figure 17: Type of element used in model discretization: PLANE183: quadratic, 8 nodes, 2D elements (Madenci & Guven, 2015)

4.2 Model geometry

Model geometry used in the model consists of two parts; the stratigraphy of the geologic column and the geometry of the salt cavern. For designing of the geologic column, it follows by the lithostratigraphy of the salt cavern location selection. For the geometry and dimension of the salt cavern is designed by using the guideline for the storage of compresses air in solution mined and salt cavities (Allen et al., 1982).

4.2.1 Salt cavern location selection

Sequestration facilities must be located relatively close to the sources of CO_2 (Dusseault et. al., 2004). Additional criteria for selecting a suitable location to develop salt caverns include: 1) the thickness of the salt layer, 2) the depth of the salt layer, and 3) temperature and pressure. A depth of greater than 800 m guarantees an environment (temperature greater than 31.1 $^{\circ}$C, pressure greater than 7.39 MPa sufficient to store CO_2 in its supercritical state or SCF where CO_2 exhibiting features of

both, gases and liquids. The benefit of storing CO_2 as SCF is the increased amount of sequestrated CO_2 due to a higher density (Bachu, 2003; Bachu & Rothenburg, 2003a).

Drill hole data from the Department of Mineral Resources (DMR), Drill hole K-89 confirms the presence of salt domes in the Ban Nong Plue, Borabue district, Maha Sarakham provinces. The stratigraphic column of K-89 is shown in figure 18. The drill hole K-89 located in Lat. 16° 00.4', Long. 103° 06.1' as shown in figure 19. The interval of K-89 from 86 to 1169 m is proven to be rock salt, interbedded with anhydrite bands (Japakasetr & Suwanich, 1982). The geothermal gradient of the salt layer is 31 °C /km (Thienprasert & Raksaskulwong, 1984). Therefore, the area around K-89 is suitable for developing salt caverns to store CO_2 in Northeast Thailand.
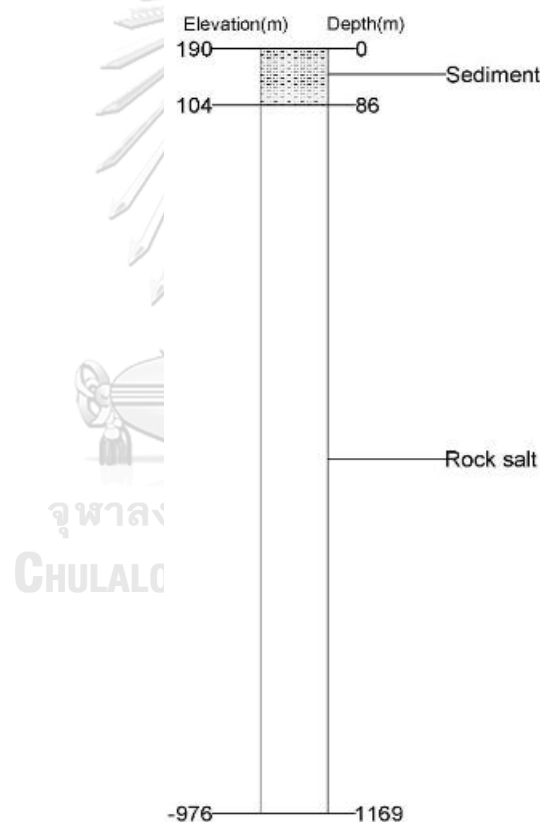
Figure 18: Stratigraphy of drill hole K-89 in the Ban Nong Plue, Borabue district, Maha Sarakham provinces. (modified from Japakasetr & Suwanich, 1982)
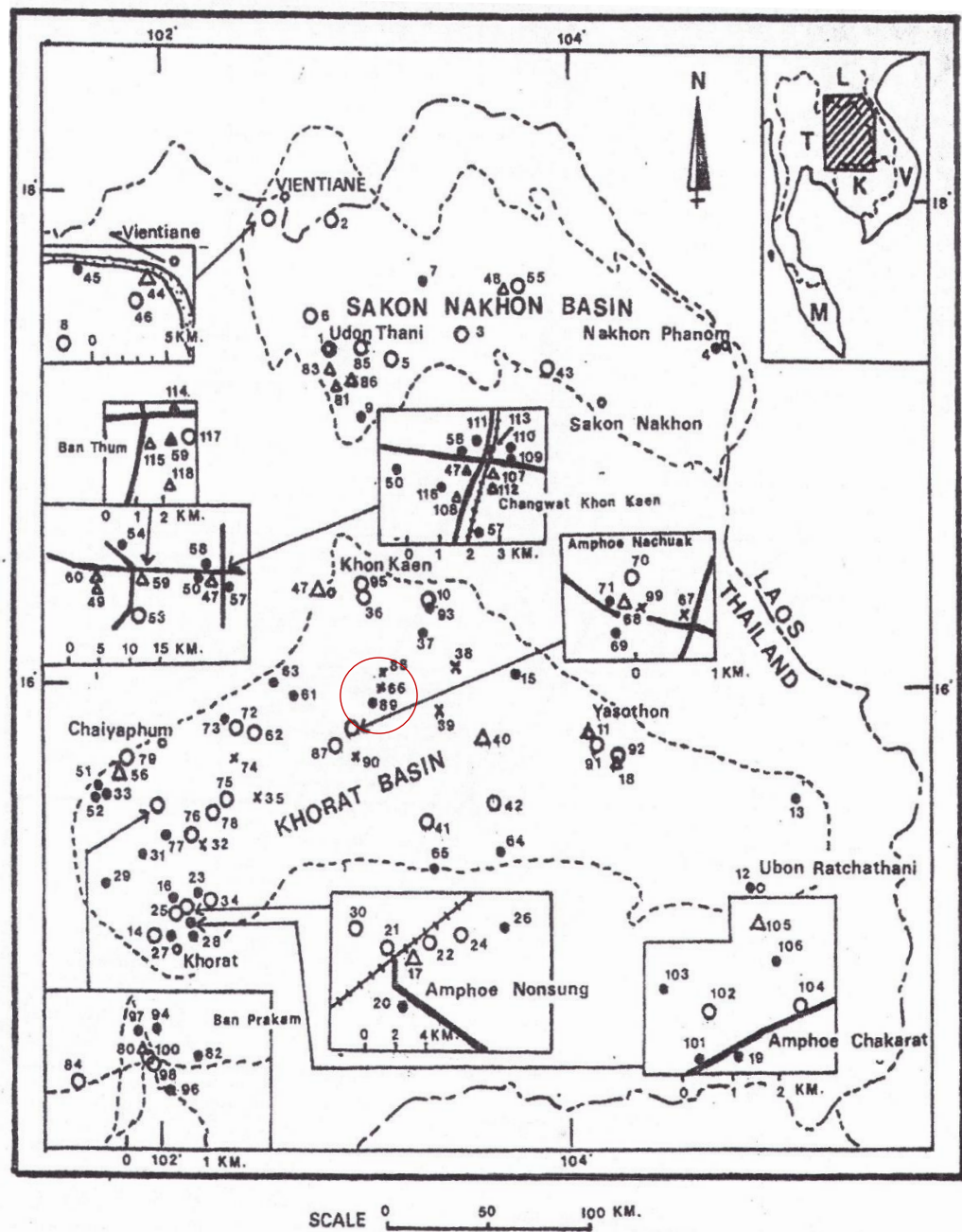
Location map of K- Drill holes (DH)

- •   DH with Rock salt
- ○   DH with Rock salt and Carnallite
- △   DH with Rock salt, Carnallite and Sylvite
- ×   Lower Rock salt and Potash Horizon did not reach

Figure 19: Location map of K-drill holes (Japakasetr & Suwanich, 1983)

4.2.2 Salt cavern geometry and dimension

The criteria used to determine which shape has the best condition for CO_2 storage are safety factor and volume change. The shape that exhibits a safety factor value greater than 1 and the lowest volume change will be considered as an optimum shape for CO_2 storage.

As shown in figure 20, the model has a width of 500 m and a total height of 1169 m. The top 86 m represent clastic sediments, while the part of the model from 86 to 1169 m, based on drill hole K-89, consists of rock salt. The centered of the designed shapes is located in the lower salt layer at 900m depth from the ground surface. For the dimension of the designed caverns used in the model is designed by using the guideline for the storage of compresses air in solution mined and salt cavities (Allen et al., 1982) are shown in figure 21.
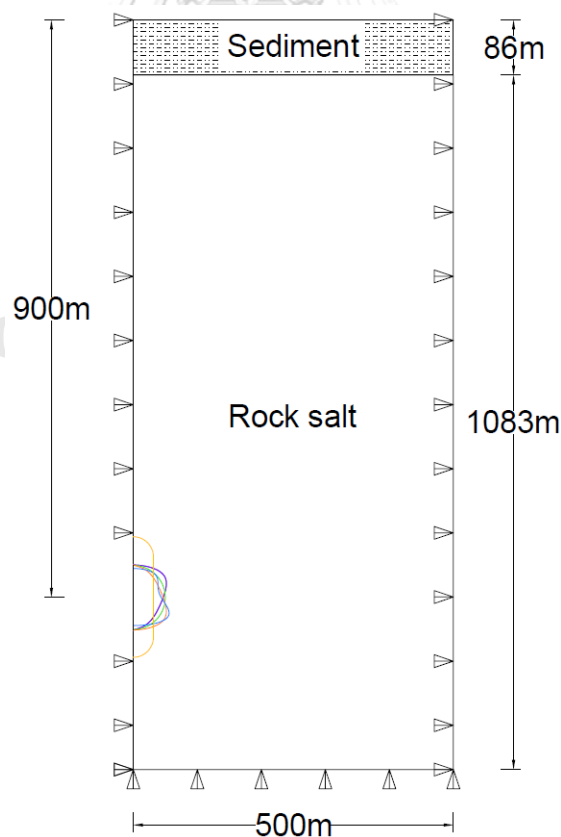
Figure 20: The model geometry and its boundary conditions used in modeling
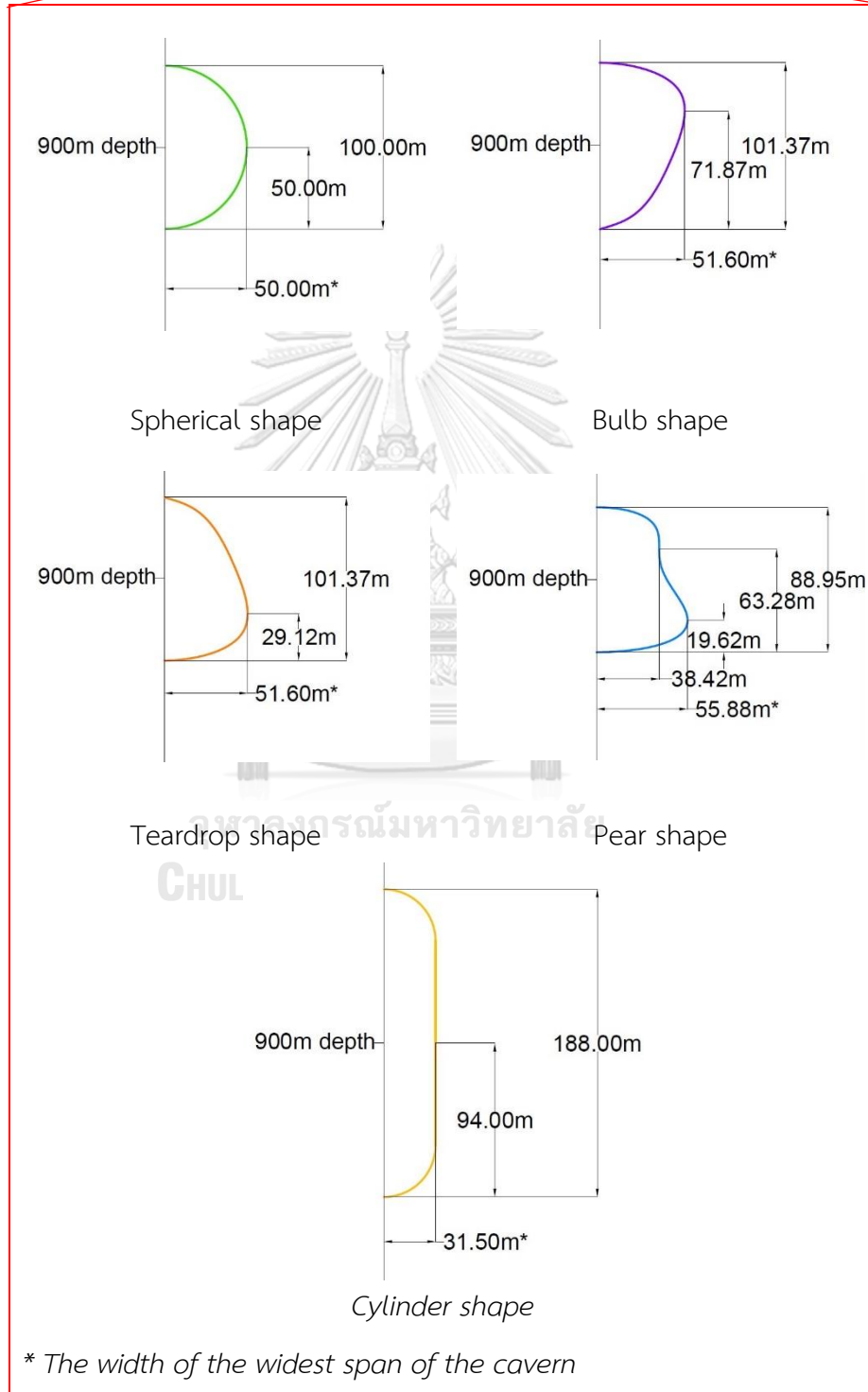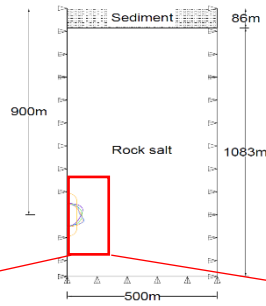
Figure 21: The designed shape cavern used in modeling

4.3 Material properties

4.3.1 Property used in the model

Material properties are one of the important factors for salt cavern design. The solid materials in the model consist of clastic sediments and rock salt. Their material properties have been retrieved from the Environmental Impact Assessment report of a Potash mining project (Asia Pacific Potash Corporation, 2014). The material properties used in our model are shown in table 1 and table 2.

Table 1: Material properties of rock salt (Asia Pacific Potash Corporation, 2014)

Material properties	Rock salt
Density (kg/m^3)	2120
Young's Modulus (GPa)	4
Poisson's Ratio	0.2
Uniaxial Compressive Strength (MPa)	29.7

Table 2: Material properties of sediments (Asia Pacific Potash Corporation, 2014)

Material properties	Sediments
Density (kg/m^3)	1750
Young's Modulus (GPa)	0.2
Poisson's Ratio	0.41

.

4.3.2 Creep parameters of Norton Creep Power law

As mentioned above, Norton Creep Power law is used to define the secondary or steady state creep stage in the model. In this research, creep parameters are obtained from the journal named "Rheology of rock salt" (Carter et al., 1993) to investigate the effect of the creep strain rate on the cavern stability. In order to select the creep parameters, five creep parameters as shown in table 3 are selected and used to model the result of displacement after the stress has been applied for 2,000 years with the temperature of 52 $^{\circ}$C where the displacement from creep trends to stable.

The criteria for choosing the creep parameters used in the model is that the selected creep parameters should give the highest magnitude of displacement among others. It means that the creep parameters that give the highest displacement will results the worst-case scenario which is happen from the creep effect of rock salt.

Table 3: The creep parameters use for modeling the displacement from creep (Carter et al., 1993)

Case	A (MPa^{-n}·s^{-1})	n	Q/R (K)
1	6.36×10^{-5}	5.93	8315
2	2.62×10^{-4}	4.31	7412
3	2.02×10^{-4}	4.52	7498
4	8.12×10^{-5}	3.42	6206
5	1.57×10^{-4}	5.34	8191

From the modeling, the highest magnitude of displacement occurs in case 4 as shown in figure 22 with the magnitude of 0.336m. Therefore, the creep parameters of case 4 are chosen for this study as shown in table 4.

จุฬาลงกรณ์มหาวิทยาลัย

CHULALONGKORN UNIVERSITY

Results of the displacement from difference creep parameters
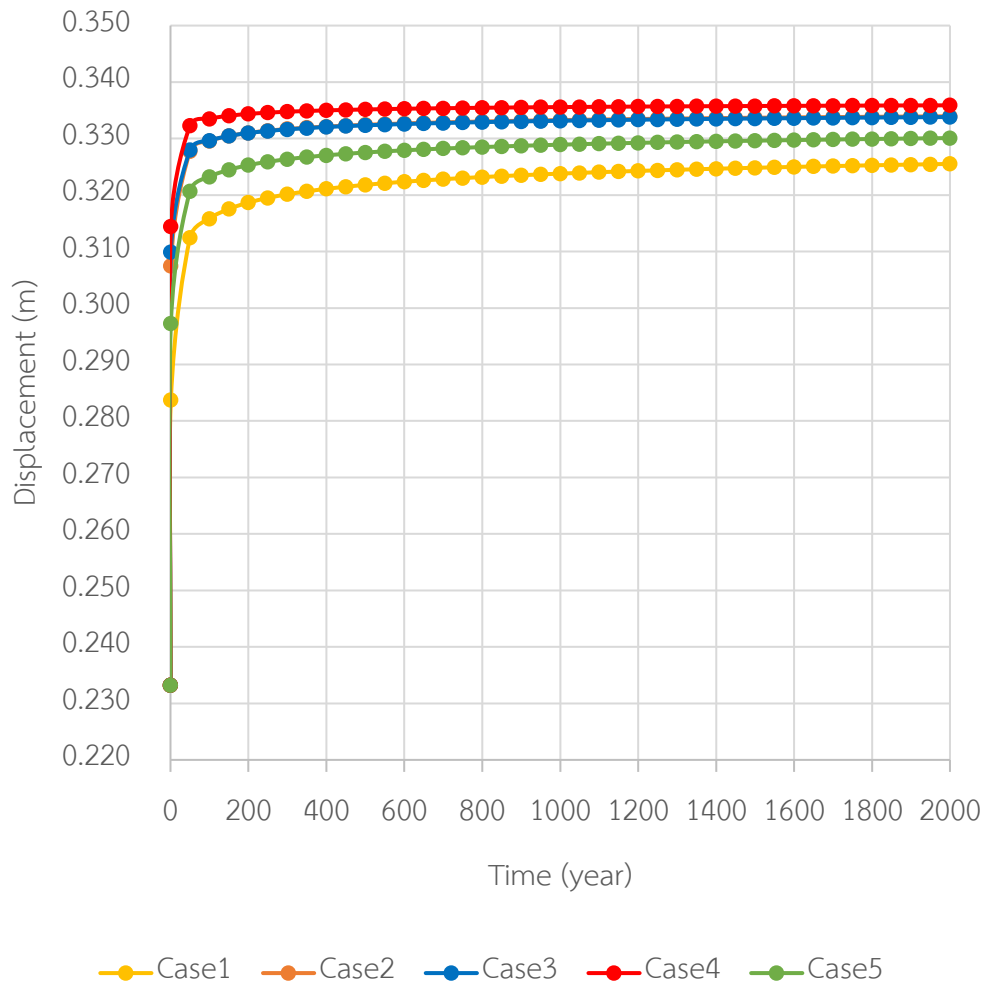
Figure 22: The results of displacement from difference creep parameters

Table 4: Creep parameters of rock salt used in the modeling (Carter et al., 1993)

Creep Parameter: Norton Creep Power Law	Rock salt
A (MPa $^{-3.42}$ ·s^{-1})	8.12×10^{-5}
n	3.42
Q (J/mol)	51,596
R (J K^{-1}mol^{-1})	8.314

4.3.3 CO_2 property

The aggregate state of the CO_2 to be filled in the rock salt cavern can be gas, liquid, or supercritical fluid. Supercritical CO_2 has a critical temperature of 31.1 $^{\circ}$C or 304.25 K, and a critical pressure of 7.39 MPa or 73.9 bar (critical point). Figure 23 shows the phase diagram of CO_2.

At 900m depth, the lithostatic pressure is 17.5 MPa and the surrounding temperature is 52 $^{\circ}$C. During the brine discharge process, CO_2 density is approximately 400 kg/m^3 and will be increased to 740 kg/m^3 before the cavern closure.
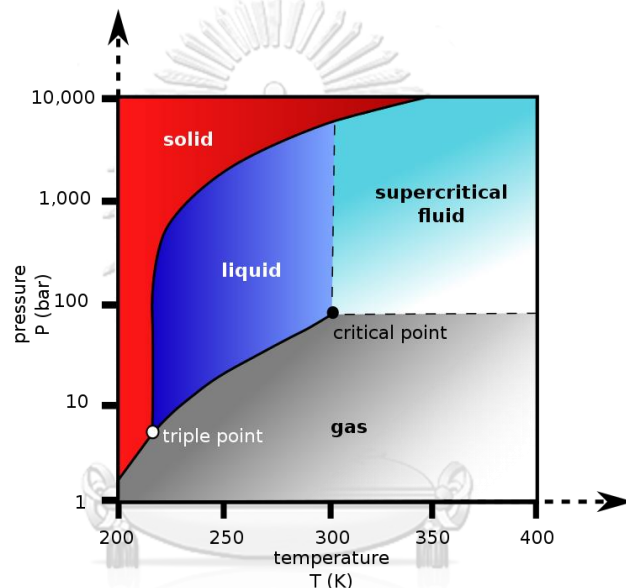
Figure 23: The phase diagram of CO_2 (Finney & Jacobs, 2010)

4.4 Salt Cavern Design, Construction and Operational Stages

The designated location for the salt cavern is the Lower Member of the Maha Sarakham Formation. The cavern is constructed by solution mining, a process during which salt is replaced by brine, over a period of 2 years (24 months). The cavern is designed as a sphere with a diameter of 100 m and would have a volume of close to 520,000 m^3. The working volume, which is the free space available for CO_2 storage, is less than the actual volume due to some brine at the bottom of the cavern which

cannot be discharged by injecting CO_2. The midpoint depth of the cavern is 900 m. The mean overburden stress is 17.84 MPa and the temperature is 52 $^\circ$C.

The pressure inside the cavern changes over time with regard to the current operational phase (Figure 24). We distinguish 4 stages: 1) solution mining, 2) discharge of the brine by injecting CO_2, 3) pre-closure CO_2 pressure adjustment and 4) cavern closure.

Stage 1 which last about 2 years (24 months) shows a pressure decrease within the cavern from 100% to 56% of the lithostatic pressure. The pressure inside the cavern is based on the hydrostatic pressure of the brine, the density of the brine being 1,180 kg/m^3 (Jeremic, 1994). During stage 2 the pressure inside the cavern is kept constant (pressure of injected CO_2 = brine pressure). After the brine is completely discharged the CO_2 pressure is adjusted pre-closure. The two common ways are: a) the pressure of the injected CO_2 is kept at brine pressure, b) the pressure of the injected CO_2 is raised to 90-95% of the lithostatic pressure. In this study, we follow the b) method as it will minimize the volume decrease (Bachu & Rothenburg, 2003b; Dusseault et al., 2004). The pressure of the injected CO_2 is raised from 56% to 95% of the lithostatic pressure during stage 3. After cavern closure (stage 4), the pressure within the cavern will remain at 95% of the lithostatic pressure.

In this research, we will investigate the salt cavern stability for a time span of 500 years after cavern closure.
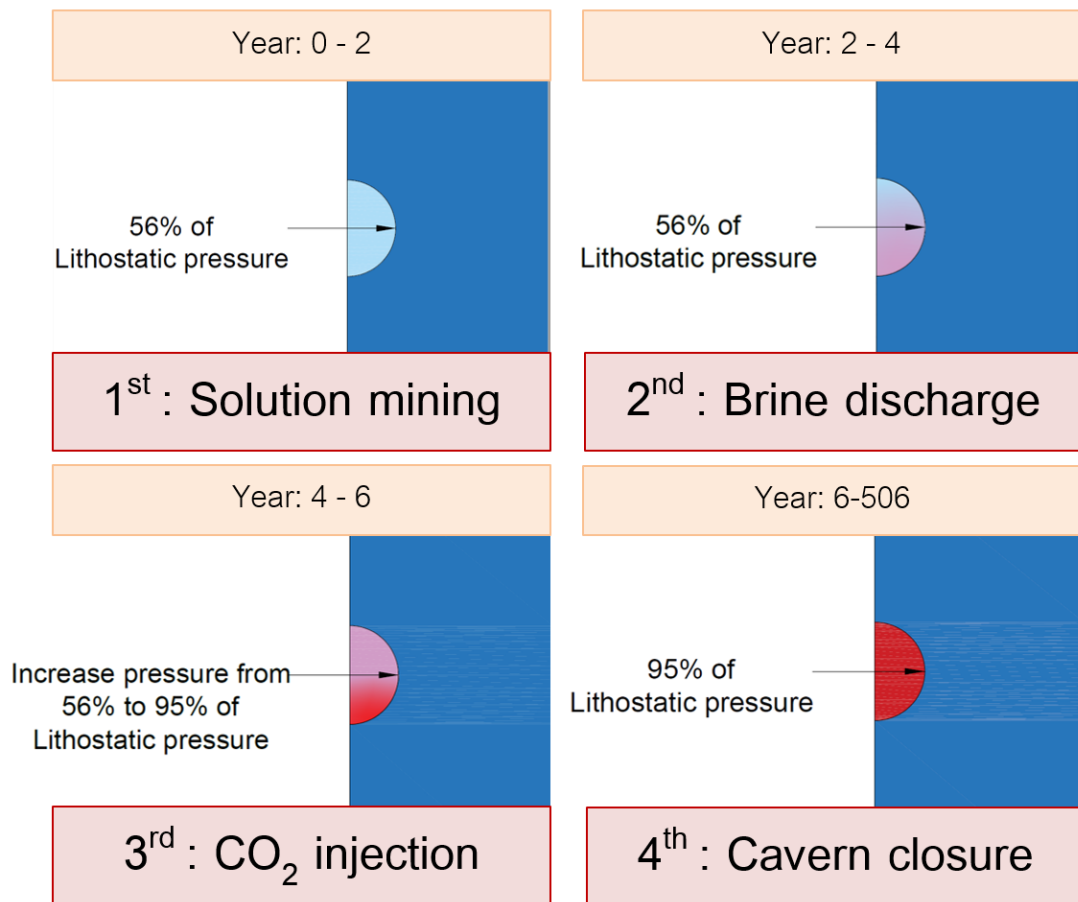
Figure 24: Modeling step of the salt cavern for CO_2 storage

CHAPTER 5

RESULTS AND DISCUSSIONS

In this research, we conduct a stability analysis of a spherical, bulb, teardrop, pear and cylindrical salt cavern, with a focus on displacement, von Mises stress, volume shrinkage, and safety factor. The results are shown in Table 5-9.

5.1 Displacement

5.1.1 Spherical shape

From table 5, the displacement vectors of the spherical shape shift inward into the cavern where the maximum magnitude of displacement in the last step of the solution mining phase is 0.459 m. In the last step of brine discharge stage, the maximum magnitude of displacement is increased to 0.505 m. After the CO_2 injection phase, the maximum magnitude of displacement decreases to 0.479 m due to the increasing of cavern pressure, and 500 years after cavern closure the maximum magnitude of displacement increases to 0.510 m because of the creep effect of rock salt. The highest magnitude of the displacement shows at the floor part of the cavern of every stage because stress that acting on the cavern's floor is the combination of the lithostatic stress and the cavern pressure. In addition, the roof of the cavern has the lowest magnitude of displacement because of the counter-balanced between the lithostatic pressure and the cavern pressure.

Table 5: Results of the spherical shape

Displacement (m)

Solution mining	Brine discharge	CO_2 injection	Cavern closure

Von Mises stress (Pa)

Solution mining	Brine discharge	CO_2 injection	Cavern closure

Safety Factor

Solution mining	Brine discharge	CO_2 injection	Cavern closure
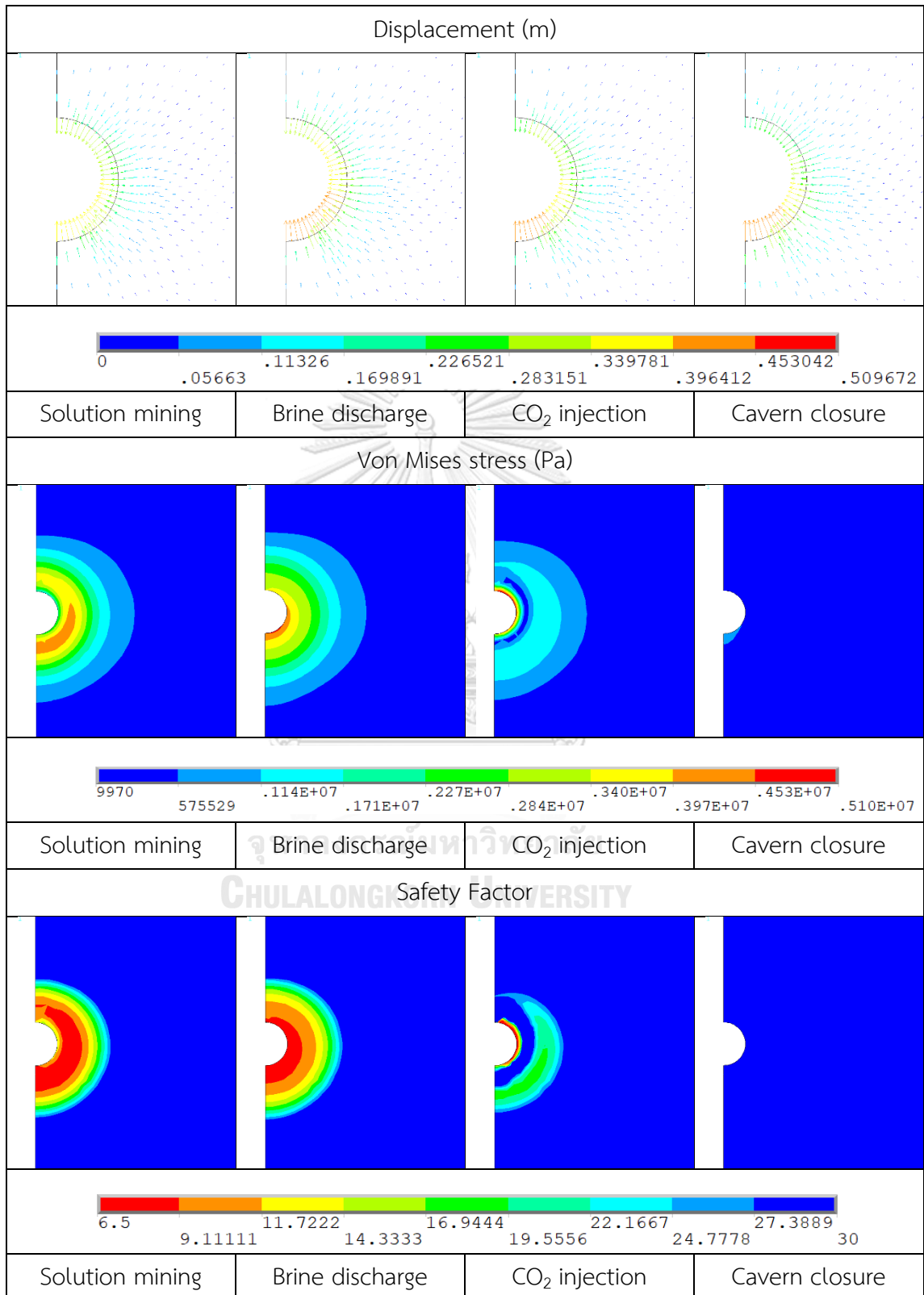
Table 6: Results of the bulb shape

Displacement (m)			
Solution mining	Brine discharge	CO_2 injection	Cavern closure
Von Mises stress (Pa)			
Solution mining	Brine discharge	CO_2 injection	Cavern closure
Safety Factor			
Solution mining	Brine discharge	CO_2 injection	Cavern closure
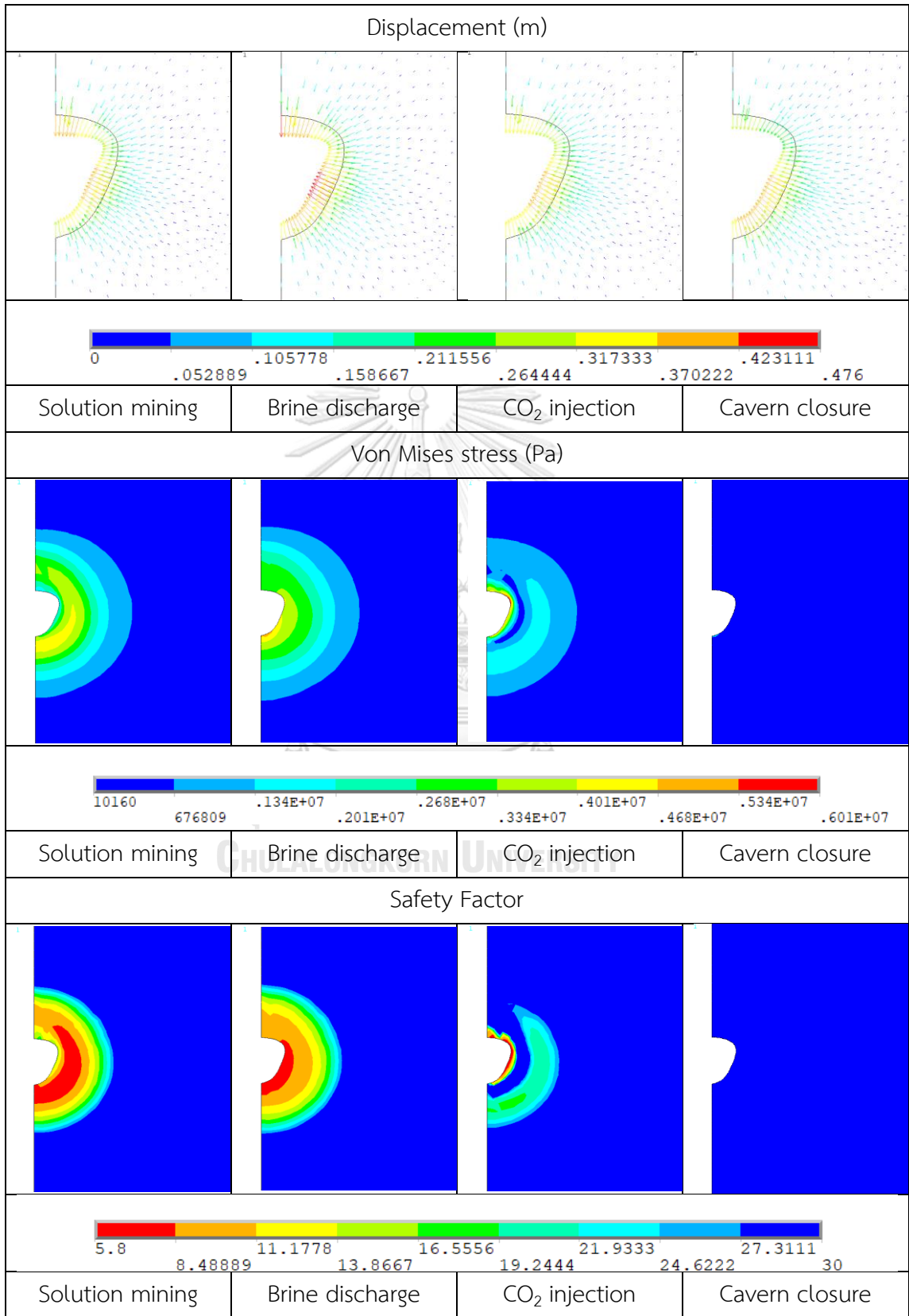
Table 7: Results of the teardrop shape

Displacement (m)			
Solution mining	Brine discharge	CO_2 injection	Cavern closure
Von Mises stress (Pa)			
Solution mining	Brine discharge	CO_2 injection	Cavern closure
Safety Factor			
Solution mining	Brine discharge	CO_2 injection	Cavern closure
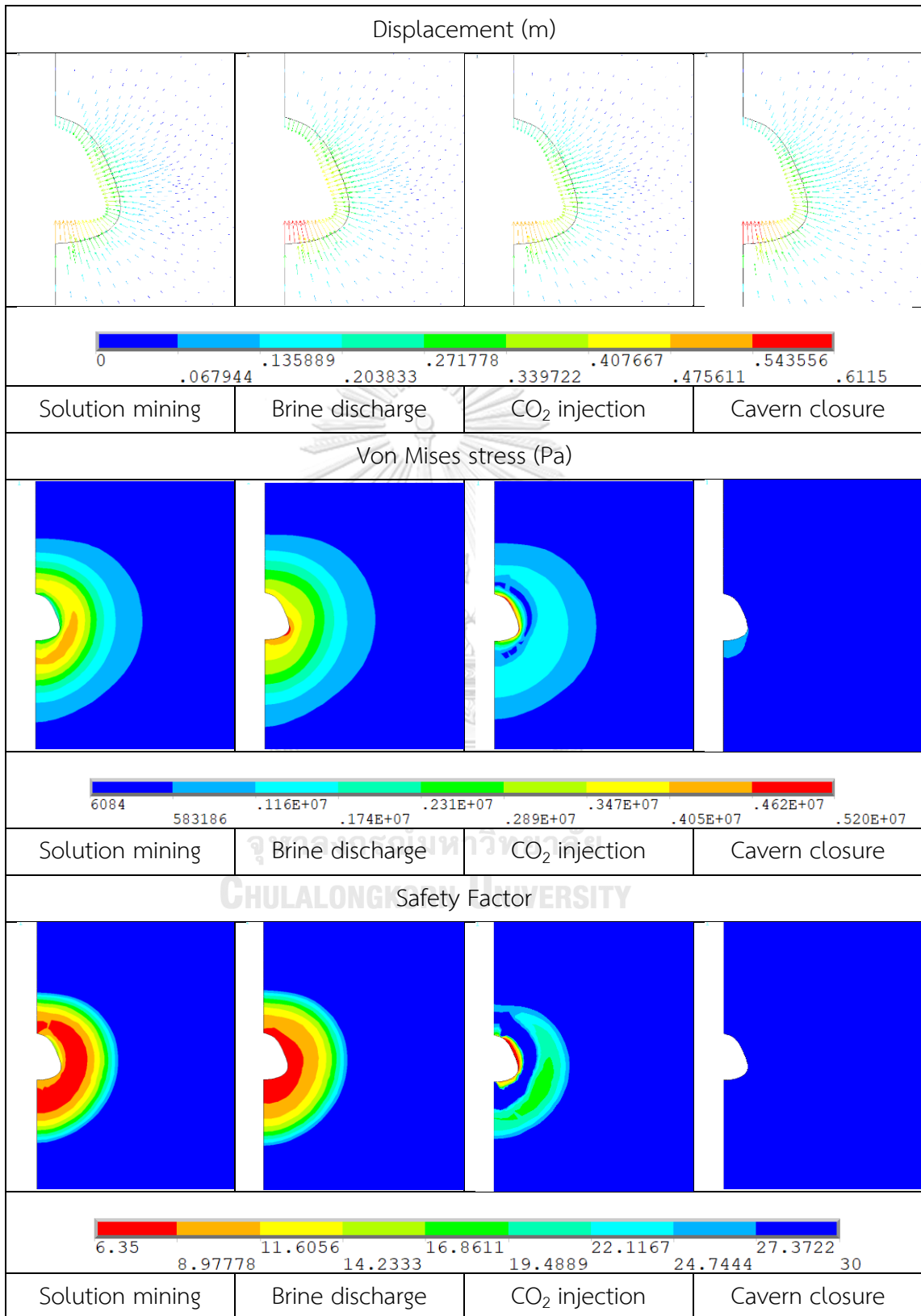
Table 8: Results of the pear shape

Displacement (m)			

Solution mining	Brine discharge	CO$_2$ injection	Cavern closure

Von Mises stress (Pa)			

Solution mining	Brine discharge	CO$_2$ injection	Cavern closure

Safety Factor			

Solution mining	Brine discharge	CO$_2$ injection	Cavern closure
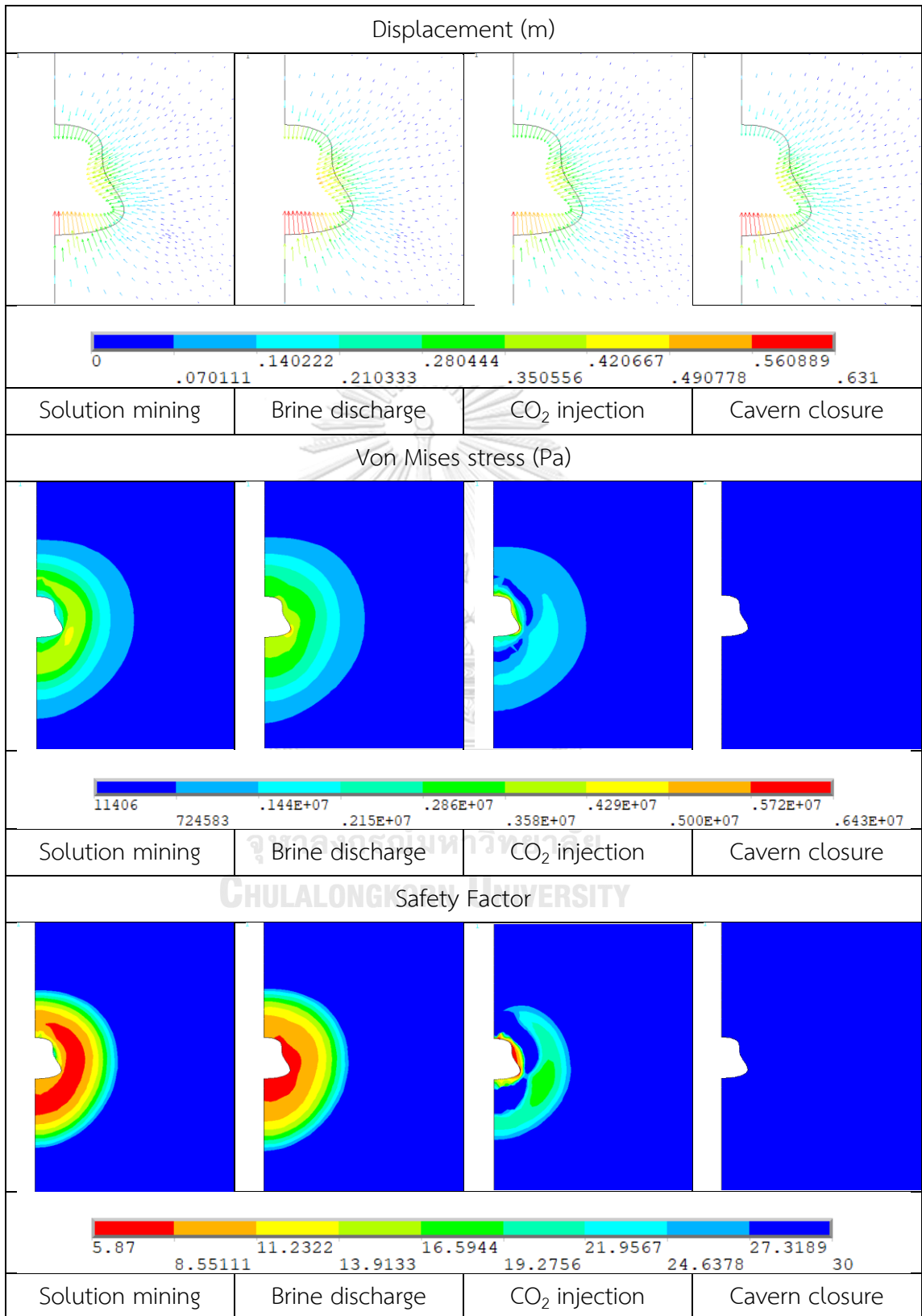
Table 9: Results of the cylindrical shape

Displacement (m)			

| Solution mining | Brine discharge | CO_2 injection | Cavern closure |
| Von Mises stress (Pa) | | | |

| Solution mining | Brine discharge | CO_2 injection | Cavern closure |
| Safety Factor | | | |

| Solution mining | Brine discharge | CO_2 injection | Cavern closure |
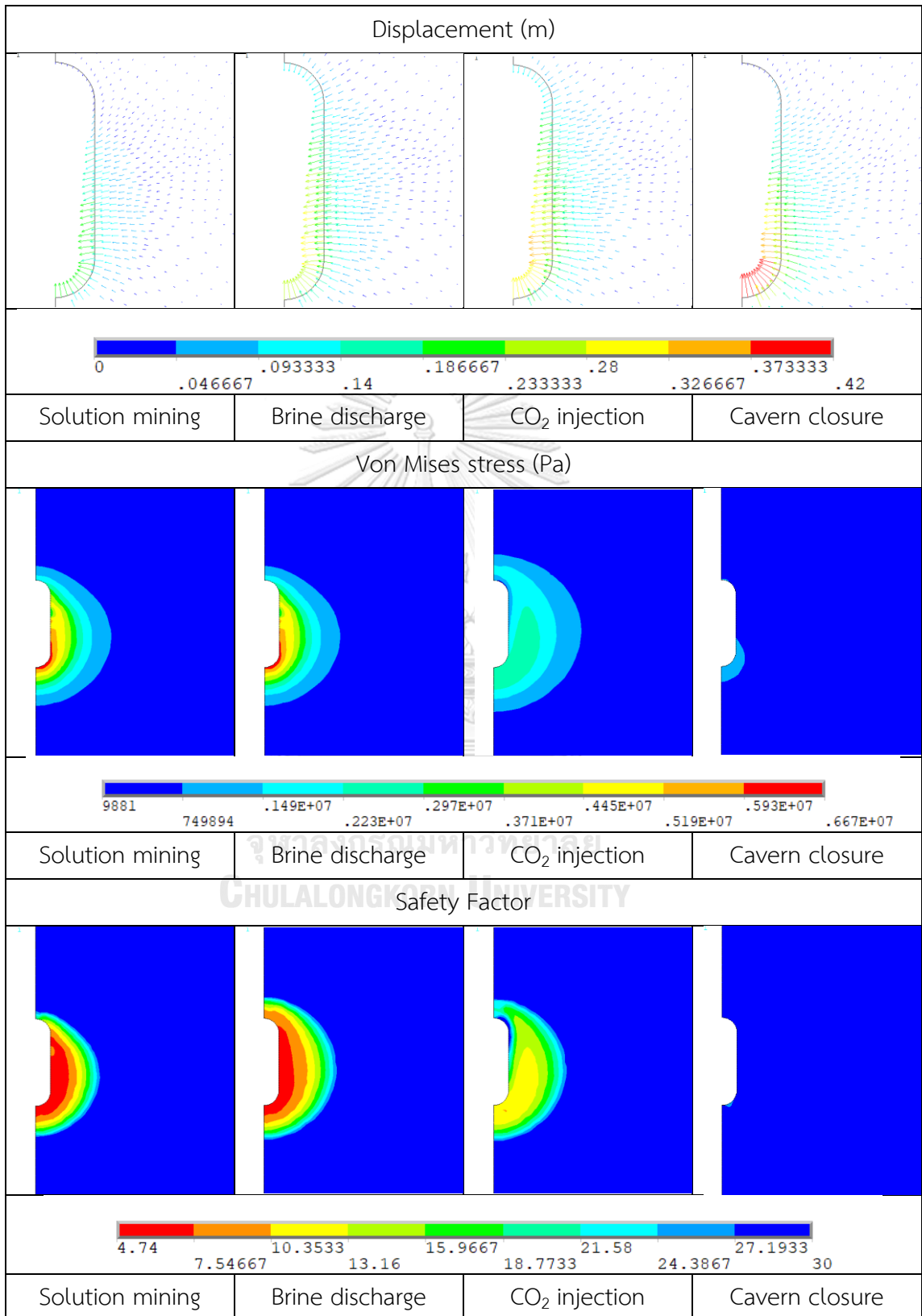
5.1.2 Bulb shape

From table 6, the displacement vectors of the bulb shaped salt cavern shift inward into the cavern where the maximum magnitude of displacement in the last step of the solution mining phase is 0.438 m. In the last step of brine discharge stage, the maximum magnitude of displacement is increased to 0.476 m. After the CO_2 injection phase, the maximum magnitude of displacement decreases to 0.444 m due to the increasing of cavern pressure, and 500 year after cavern closure, the maximum magnitude of displacement increases to 0.462 m because of the creep effect of rock salt. The highest magnitude of the displacement shows at the wall of the cavern in every stage because the geometry of the cavern. The wall of bulb shaped cavern is straight which make the stress concentrate at the cavern's wall.

5.1.3 Teardrop shape

From table 7, the displacement vectors of the teardrop shape shift inward into the cavern where the maximum magnitude of displacement in the last step of the solution mining phase is 0.559 m. In the last step of brine discharge stage, the maximum magnitude of displacement is increased to 0.611 m. After the CO_2 injection phase, the maximum magnitude of displacement decreases to 0.569 m due to the increasing of cavern pressure, and 500 year after cavern closure is the maximum magnitude of displacement increases to 0.608 m due to the creep effect of rock salt. The highest magnitude of the displacement shows at the floor part of the cavern of every stage because stress that acting on the cavern's floor is the combination of the lithostatic stress and the cavern pressure. But, when compare the maximum magnitude of displacement between teardrop shape and spherical shape, it shows that the teardrop shape gives the higher value of displacement magnitude because the floor of the teardrop is straighter than the spherical shape.

5.1.4 Pear shape

From table 8, the displacement vectors of the pear shape shift inward into the cavern where the maximum magnitude of displacement in the last step of the solution mining phase is 0.572 m. In the last step of brine discharge stage, the maximum magnitude of displacement is increased to 0.631 m. After the CO_2 injection phase, the maximum magnitude of displacement decreases to 0.576 m due to the increasing of cavern pressure, and 500 year after cavern closure is the maximum magnitude of displacement increases to 0.609 m due to the creep effect of rock salt. The highest magnitude of the displacement shows at the floor part of the cavern of every stage. At the wall of the cavern shows the intermediate movement because of the acute curve which made the stress concentrate in this area.

5.1.5 Cylindrical shape

From table 9, the displacement vectors of the cylindrical cavern shift inward into the cavern where the maximum magnitude of displacement in the last step of the solution mining phase is 0.328 m. In the last step of brine discharge stage, the maximum magnitude of displacement is decreased to 0.322 m, and the CO_2 injection phase, the maximum magnitude of displacement increases to 0.345 m which differs from others which could be the result of the cavern's geometry, where the span of the cavern is lesser, and the height of the cavern is higher when compares with other shapes. Therefore, the range of lithostatic pressure acting on the cavern is wider when compared to other shapes. For 500 year after cavern closure, the maximum magnitude of displacement increases to 0.419 m because of the creep effect of rock salt. The highest magnitude of the displacement shows at the floor of the cavern in every stage because of the combination of the lithostatic stress and the cavern pressure.

To summarize, the displacement vector results show that the direction of the vectors shifts inward the salt cavern. The highest magnitude of the displacement shows at the floor part of all designed salt cavern shapes, except the bulb shape

where the highest magnitude is at the wall of the cavern. The highest magnitude of the displacement mostly happened during brine discharge (stage 2) and displacement magnitude tends to decrease after CO_2 injection (stage 3) and increased again after the cavern closure due to the creep behavior of rock salt.

5.2 Von Mises stress

5.2.1 Spherical shape

From table 5, the maximum of Von Mises stress in the last step of the solution mining phase is 4.26 MPa and increased to 4.67 MPa which shows at the cavern's floor after the brine discharge stage. After the CO_2 injection phase, the maximum of Von Mises stress increase to 5.09 MPa which is the result from the differential stress increased while injecting the CO_2 into the cavern. For 500 year after cavern closure, the maximum of Von Mises stress decreases to 0.70 MPa because the adaptation of pressure inside the cavern in order to make it as same as the surrounding pressure. But, the differential stress, the light blue contour at the cavern floor, still remain after the 500 years cavern closure so it could imply that the development of the pressure inside the cavern to be the same as the surroundings is slow.

5.2.2 Bulb shape

From table 6, the maximum of Von Mises stress in the last step of the solution mining phase is 4.45 MPa and increased to 5.01 MPa which shows at the cavern's floor after the brine discharge stage. After the CO_2 injection phase, the maximum of Von Mises stress increase to 6.00 MPa which is the result from the differential stress increased while injecting the CO_2 into the cavern (the same reason as spherical shape). For 500 year after cavern closure, the maximum of Von Mises stress decreases to 0.71 MPa, where the differential stress is reduced, causing the creep rate to slow.

5.2.3 Teardrop shape

From table 7, the maximum of Von Mises stress in the last step of the solution mining phase is 4.30 MPa and increased to 4.97 MPa after the brine discharge stage. The maximum of Von Mises stress shows at the cavern's floor at the acute curve where stresses are concentrated in this area. After the CO_2 injection phase, the maximum of Von Mises stress increase to 6.00 MPa which is the result from the differential stress increased while injecting the CO_2 into the cavern (the same reason as spherical and teardrop shape). For 500 year after cavern closure, the maximum of Von Mises stress decreases to 0.71 MPa. Where the highest value is at the cavern floor because the slow development of the pressure inside the cavern to be the same as the surroundings. Therefore, the differential stress, the light blue contour, still remain after the 500 years cavern closure.

5.2.4 Pear shape

From table 8, the maximum of Von Mises stress in the last step of the solution mining phase is 4.48 MPa and increased to 5.57 MPa which shows at the acute curve of the cavern's floor after the brine discharge stage. After the CO_2 injection phase, the maximum of Von Mises stress increase to 6.42 MPa which is the result from the differential stress increased while injecting the CO_2 into the cavern. For 500 year after cavern closure, the maximum of Von Mises stress decreases to 0.73 MPa, where the differential stress is reduced.

5.2.5 Cylindrical shape

From table 9, the maximum of Von Mises stress in the last step of the solution mining phase is 6.66 MPa and decreased to 6.31 MPa after the brine discharge stage. The maximum of Von Mises stress shows at the cavern's floor at the acute curve where stresses concentration is high in this area. After the CO_2 injection phase, the maximum of Von Mises stress decrease to 2.97 MPa. For 500 year after cavern closure, the maximum of Von Mises stress decreases to 1.25 MPa. Where the highest

value is at the cavern floor because the slow development of the pressure inside the cavern to be the same as the surroundings. Therefore, the differential stress, the light blue contour, still remain after the 500 years cavern closure. When compared the Von mises stress results of cylindrical shape and other shapes, the cylindrical shape differs from others because the Von Mises stress tend to decrease at the end of every operation stage. The reason could be the wide range of lithostatic pressure acting on the cavern made the differential stress reduced.

To summarize, the process of CO_2 sequestration in salt caverns affects the stress field. Before the start of the cavern construction, the prevailing stress field (virgin stress) was dominated by the lithostatic pressure. During and after the excavation process, a disturbance of the stress field can be recognized caused by solution mining and brine discharge and the associated difference between stress and cavern pressure (56% of the lithostatic pressure). Where the highest stress happened in this stage, mostly at the bottom part of the cavern in every cavern shape. Due to the injection of CO_2 at high pressure (95% of the lithostatic pressure) this difference is diminished, causing the creep rate to slow, and ultimately the virgin stress is approached asymptotically.

5.3 Safety factor

The safety factor is used to describe the stability of the cavern. In our models, the safety factor is based on the ratio between rock strength (Uniaxial Compressive Strength) and Von Mises stress. Therefore, the trend of the safety factor would be the same as the Von Mises stress. A structure is considered to be safe if the safety factor has a value greater than 1. The lowest safety factor value in every shape, except for the cylindrical shape, shows in the CO_2 injection phase where 6.53, 5.58, 6.35, and 5.87 are the lowest safety factor values for spherical, bulb, teardrop, and pear shape respectively. For the cylindrical shape, the lowest safety factor value shows in the solution mining phase which has a value of 4.74. The shape exhibiting the highest safety factor value is the spherical shape while the cylindrical shape

shows the lowest value for the safety factor of all modeled shapes. The cylindrical shape is nevertheless still considered as safe for CO_2 storage. Consequently, based on our modeling results, salt caverns can be considered a safe option for CO_2 storage in its supercritical state.

5.4 Volume change

As shown in figure 25, the highest volume change in spherical, bulb, teardrop, and pear shape occurred during the brine discharge stage. For the cylindrical shape, the highest volume change is at the CO_2 injection phase. 500-years after cavern closure, volume shrinkage happens in the teardrop and cylindrical shape with the value of 0.018% and 0.604%, respectively. Contrary, the volume of the pear, spherical, and bulb shaped caverns expand by 0.023%, 0.061%, and 0.151%, respectively. From the criteria of designing the cavern shapes with the same amount of volume of designed caverns, the results show that the lowest volume change of the cavern is teardrop, following by pear, spherical, bulb, and cylindrical shape, respectively.

Figure 26 illustrates the difference in the upper part dimension of teardrop, spherical, and bulb shape. From comparing the teardrop, spherical, and bulb shape which have the same cavern height, but differ in the width in the upper part of the cavern. It can explain that if the upper part of the cavern is wider, the volume change will increase.

In addition, if the height of the cavern is increased, the volume change tends to be increased as the cylindrical shape has the highest height (approximate of 180 m height) among others (approximately 100 m height). In addition, the height has more influence on the volume change than the upper part of the cavern height. As the upper part of pear shape and spherical shape width is nearly the same, but the pear shape has the less height compared to the spherical shape so that the volume change of pear is lower than the spherical shape.
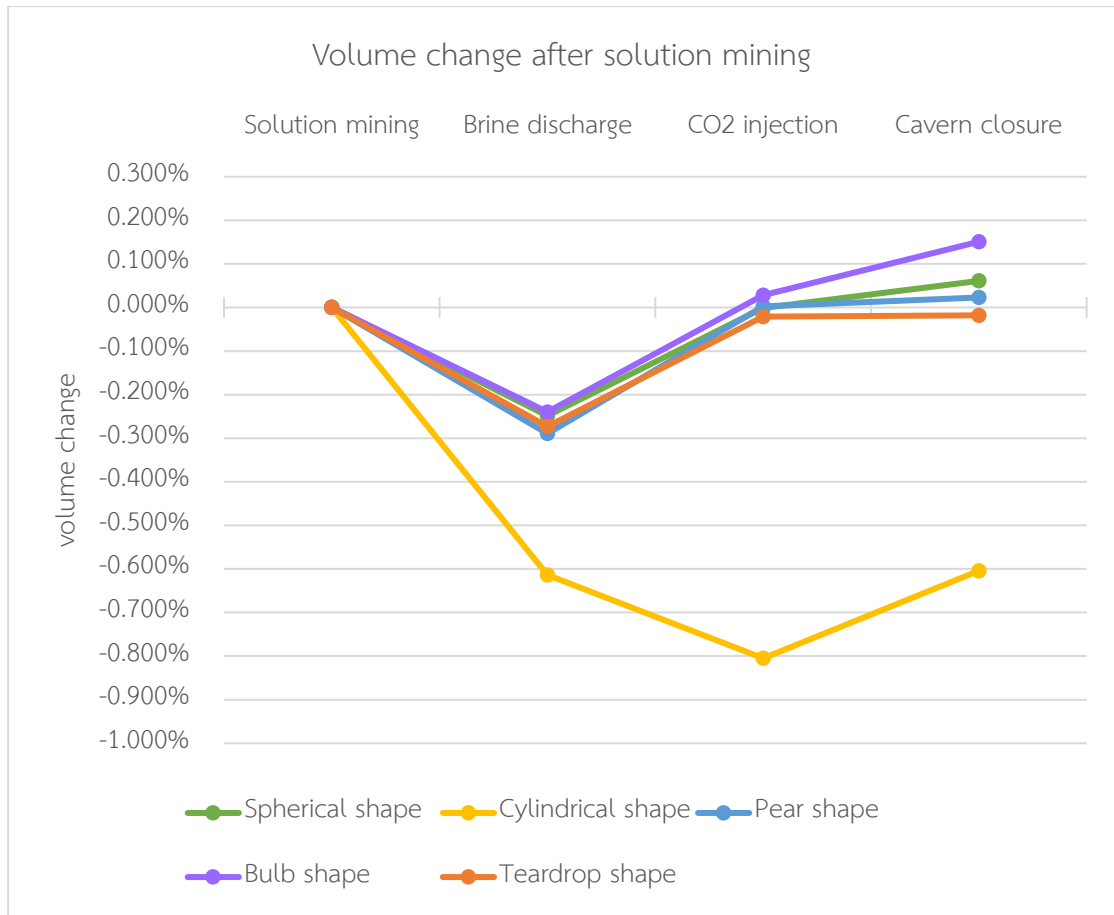
Figure 25: Volume change after solution mining of each shape.
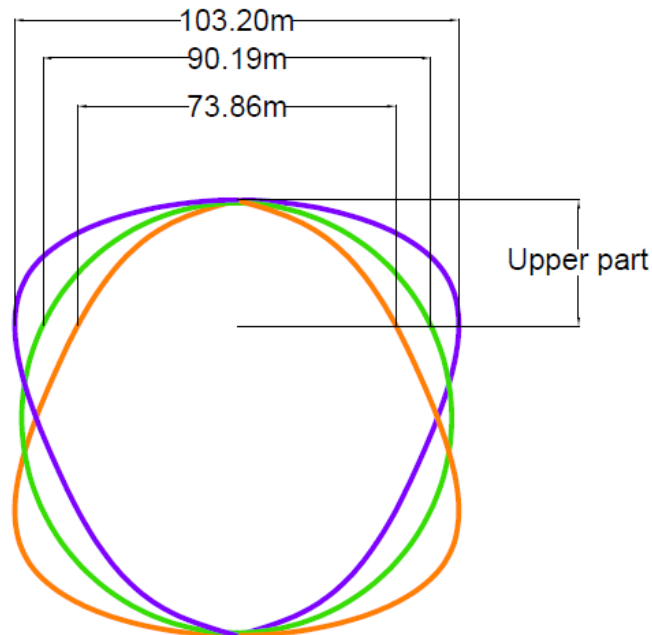
Figure 26: The width dimension of the teardrop, bulb, spherical shape cavern at the upper part cavern.

5.5 Ground subsidence

Ground subsidence is a critical value for local communities, as it affects their lives directly, leading to damage of infrastructure and housing. As results of subsidence which focus on the top surface of the model, the maximum subsidence of each shape is shown in Table 10.

Table 10: Maximum subsidence of the top surface in each shape

Stage	Maximum subsidence of the top surface in the model (cm)				
	Spherical	Bulb	Teardrop	Pear	Cylindrical
Solution mining	0.75	0.75	0.81	0.88	0.39
Brine discharge	0.86	0.86	0.93	1.01	0.54
CO_2 Injection	0.69	0.68	0.75	0.80	0.42
Cavern closure	1.84	1.79	1.99	2.07	1.51

In the operation stages, the trend of the subsidence increases due to the cavern pressure decreases in solution mining and brine discharge stage even though the pressure inside the cavern in brine discharge stage is kept the same pressure as solution mining at 56% of lithostatic pressure which is the effect from the rock salt behavior, creep properties. After the CO_2 injection, the subsidence is decreased from the increasing of cavern pressure that interact with the lithostatic pressure in the different direction (counter-balanced), whereas the subsidence trends to increase after the cavern closure because of the creep properties. Moreover, the maximum of subsidence occurs at the stage after 500 years cavern closure, where pear shape has the maximum subsidence value of 2.07 cm. On the other hand, cylindrical shape has the least ground subsidence (1.51 cm) among the investigate shapes.

Due to the depth of the cavern, the maximum magnitude of ground subsidence predicted in the models is approximately 2 cm within the time span of 500 years can be considered insignificant and have no adverse effect on the surrounding environments and local communities (Vattanasak, 2006).

5.6 Amount of CO_2 storage

From the geomechanical modeling, 0.4 million ton of CO_2 in Supercritical fluid state can be kept in 520,000 m^3 salt cavern. Therefore, at least five salt caverns are needed to store all the CO_2 emitted from the natural gas power plant in Northeast Thailand which emits 2 million tons of CO_2 per year.

5.7 The optimum shape for CO_2 storage

The criteria used to determine which shape has the best condition for CO_2 storage are safety factor and volume change. Where the ground subsidence will not be used as a criterion because the result of ground subsidence predicted from the models is approximately 2 cm which is negligible (Vattanasak, 2006).

For the safety factor, if the lowest safety factor of the cavern in every stage is greater than or equal to 4 which is the recommended value for the structure using under the difficult and environmental conditions (Maria, 2016), it will be selected as

a candidate for finding the optimal shape and treated the same as the shape that its safety factor is greater than 4. Moreover, the shape that exhibits the lowest volume change will be considered as an optimum shape for CO_2 storage. In this case study, the teardrop shape is the optimum shape for storing CO_2 in its supercritical state. Its safety factor value is greater than 4 and it exhibits the lowest volume change of all investigated shapes as shown in table 11.

Table 11: Comparison of the results between all investigated shapes

Shape	Safety factor	Volume Change [*]	Ground Subsidence
Teardrop	6.35	-0.018%	1.99 cm
Pear	5.87	0.023%	2.07 cm
Spherical	6.53	0.061%	1.84 cm
Bulb	5.85	0.151%	1.79 cm
Cylindrical	4.74	-0.604%	1.51 cm

* (-) for volume decrease

(+) for volume increase

CHAPTER 6

CONCLUSION

6.1 Conclusion

The Maha Sarakham Formation exhibits very thick rock salt layers, especially the Lower Member. The area in the vicinity of drill hole K-89 is ideally suited for the storage of CO_2 in salt caverns in its supercritical fluid state (SCF).

The modeling results show that the salt cavern stability is ensured for a time span of at least 500 years. All the designed shapes have a safety factor value greater than 4, making them technically viable for being used as a Carbon Dioxide Storage. The optimum shape for storing CO_2 in its supercritical fluid state, maximizing the cavern stability is the teardrop shape with a safety factor value of 6.36, also exhibiting the lowest volume change (-0.018%) of all investigated shapes. Ground subsidence is insignificant. 0.4 million ton of CO_2 in supercritical fluid state can be kept within the 520,000 m^3 salt cavern. Therefore, at least five salt caverns are needed to store all the CO_2 emitted from the natural gas power plant in Northeast Thailand. The sequestration process is shown to be safe and negative effects on the local communities improbable.

This study shows that storage of CO_2 in salt caverns in Northeast Thailand is a technically viable and safe solution for the reduction of anthropogenic CO_2 emissions into the atmosphere.

6.2 Recommendation

1. Optimizing the layout for multiple storage caverns should be considered in future studies, ensuring the long-term stability of all the caverns.
2. Including a well bore casing stability analysis is recommend for future studies, since the well bore stability is also important during the operation of a CO_2 storage facility.

3. Constitutive creep laws of primary and tertiary creep stages could be included, making the model parameters more realistic.

4. Optimizing the salt cavern for shallow depths (less than 800m depth), CO_2 not being in its supercritical fluid state.

REFERENCES

Allen, R. D., Doherty, T. J., & Thoms, R. L. (1982). Geotechnical factors and guidelines for storage of compressed air in solution-mined salt cavities. doi:10.2172/5234728

Asia Pacific Potash Corporation. (2014). *Environmental Impact Assessment (Final report) for Potash Mine Project*. Retrieved from

Bachu, S. (2003). Screening and Ranking Sedimentary Basins for Sequestration of CO2 in Geological Media in Response to Climate Change. *Environmental Geology, 44(3)*, 277-289. doi:10.1007/s00254-003-0762-9

Bachu, S., & Rothenburg, L. (2003a). *Carbon dioxide sequestration in salt caverns: capacity and long term fate*.

Bachu, S., & Rothenburg, L. (2003b). Carbon dioxide sequestration in salt caverns: capacity and long term fate.

Boonyatee, T. *Outline of FEM procedures : 6 Steps of FEM, lecture notes, Chulalongkorn University*.

Carter, N. L., Horseman, S. T., Russell, J. E., & Handin, J. (1993). Rheology of rocksalt. *Journal of Structural Geology, 15*(9), 1257-1271. doi:https://doi.org/10.1016/0191-8141(93)90168-A

Choomkong, A., Sirikunpitak, S., Darnsawasdi, R., & Yordkayhun, S. (2017). A study of CO2 Emission Sources and Sinks in Thailand. *Energy Procedia, 138*, 452-457. doi:https://doi.org/10.1016/j.egypro.2017.10.198

Costa, A., Amaral, C., Poiate Jr, E., Pereira, A., Martha, L., Gattass, M., & Roehl, D. (2011). *Underground storage of natural gas and CO2 in salt caverns in deep and ultra-deep water offshore Brazil*.

Costa, P., Roehl, D., Costa, A., Amaral, C., & Poiate Jr, E. (2014). *Underground salt caverns opened by solution mining for brine production and storage of natural gas*.

Divedi, H. (2017). DEFINE POISSON'S RATIO IN PHYSICS. Retrieved from https://www.hkdivedi.com/2017/01/define-poissons-ratio-in-physics.html

Dusseault, M. B., Bachu, S., & Rothenburg, L. (2004). Sequestration of CO2 in salt

caverns. *Journal of Canadian Petroleum Technology, 43*(11), 49-55.

Dusseault., M. B., Bachu., S., & Davidson., B. C. (2001). *Carbon Dioxide Sequestration Potential in Salt Solution Caverns in*

Alberta, Canada. Paper presented at the Solution Mining Research Institute, Fall 2001 Technical Meeting, Albuquerque, New Mexico, USA.

El Tabakh, M., Utha-Aroon, C., & Schreiber, B. C. (1999). Sedimentology of the Cretaceous Maha Sarakham evaporites in the Khorat Plateau of northeastern Thailand. *Sedimentary Geology, 123*(1-2), 31-62.

Energy Policy and Planning Office. (2018). CO_2 Emission from Energy Consumption by Sector. . Retrieved from http://www.eppo.go.th/epposite/images/Energy-Statistics/energyinformation/Energy_Statistics/Emission/T09_01_03-2.xls

Feunkajorn, K. (2013). *Performance assessment of rock salt formation in the northeast of Thailand for CO_2 storage* (SUT7-719-55-24-32). Retrieved from http://sutir.sut.ac.th:8080/sutir/handle/123456789/4595

Finney, B., & Jacobs, M. (2010). In P. d. o. C. c. dioxide) (Ed.), *Commons, Image:Carbon dioxide pressure-temperature phase diagram.jpg*.

Groenefeld, P., Yoshida, Y., Koder, M., & Bunpapong, T. (1993). *Four Years of Brine Production by Solution Mining: The Pimai Project in Thailand.* Paper presented at the 7th Symposium on Salt, Kyoto, Japan.

Hudson, J., & Harrison, J. (2000). *Engineering Rock Mechanics: An Introduction to the Principles 1st Edition*. Amsterdam: Pergamon.

Japakasetr, T., & Suwanich, P. (1982). *Potash and Rock salt in Thailand: Appendix A*. Retrieved from Bangkok, Thailand:

Japakasetr, T., & Suwanich, P. (1983). *Potash and Rock salt in Thailand: Appendix F: Showing Locations Map of Drill Holes*. Retrieved from Bangkok, Thailand:

Jeremic, M. L. (1994). *Rock mechanics in salt mining*. Rotterdam: Balkema.

K-UTEC- Sondershausen. Solution mining Retrieved from https://www.k-utec.de/fileadmin/redakteur/CPV/Dokumente/Solution_mining_03.ppt

Kohnhe, P. (2013). *ANSYS Mechanical APDL Theory Reference 15*. Retrieved from U.S.A:

Madenci, E., & Guven, I. (2015). *The Finite Element Method and Applications in*

Engineering Using Ansys®: Springer US.

Maria, R. (2016). *SUMMARY OF SAFETY CRITERIA IN DESIGN*.

Mehta, F., & Joshi, H. (2016). Finite Element Method: An Overview. *IOSR Journal of Dental and Medical Sciences (IOSR-JDMS), 15*(3), 38-41. doi:10.9790/0853-15333841

Mraz, D. (1980). Plastic behavior of salt rock utilized in designing a mining method. *CIM Bull, 3*, 115–123.

Park, S.-S. (2010). Effect of Wetting on Unconfined Compressive Strength of Cemented Sands. *Journal of Geotechnical and Geoenvironmental Engineering - J GEOTECH GEOENVIRON ENG, 136*. doi:10.1061/(ASCE)GT.1943-5606.0000399

Shi, J. Q., & Durucan, S. (2005). CO_2 storage in caverns and mines. *Oil & Gas Science and Technology-Revue D Ifp Energies Nouvelles, 60*(3), 569-571.

Spaceflight.esa.int. (2019). IMPRESS Education: Mechanical Properties, Testing. Retrieved from http://www.spaceflight.esa.int/impress/text/education/Mechanical%20Properties/Question_Mechanical_Properties_24.html

Thienprasert, A., & Raksaskulwong, M. (1984). Heat flow in northern Thailand. *Tectonophysics, 103*(1), 217-233. doi:https://doi.org/10.1016/0040-1951(84)90085-4

Utha-Aroon, C. (1993). Continental origin of the Maha Sarakham evaporites, northeastern Thailand. *Journal of Southeast Asian Earth Sciences, 8*(1), 193-203. doi:https://doi.org/10.1016/0743-9547(93)90021-G

Value design Consulting. (2019). FEA Stress Theories. Retrieved from http://www.value-design-consulting.co.uk/stress-theories.html

Vattanasak, H. (2006). *Salt reserve Estimation For Solution Mining in The Khorat Basin.* (Degree of Master of Engineering in Geotechnology), Suranaree University of Technology, Retrieved from http://sutir.sut.ac.th:8080/sutir/handle/123456789/1072

Wang, T., Yan, X., Yang, H., Yang, X., Jiang, T., & Zhao, S. (2013). A new shape design method of salt cavern used as underground gas storage. *Applied Energy, 104*, 50-61. doi:https://doi.org/10.1016/j.apenergy.2012.11.037

Yang, C., Wang, T., Li, Y., Yang, H., Li, J., Qu, D. a., . . . Daemen, J. J. K. (2015). Feasibility analysis of using abandoned salt caverns for large-scale underground energy storage in China. *Applied Energy, 137*, 467-481. doi:https://doi.org/10.1016/j.apenergy.2014.07.048

จุฬาลงกรณ์มหาวิทยาลัย
CHULALONGKORN UNIVERSITY

VITA

NAME   Narumas Pajonpai

DATE OF BIRTH   17 January 1995

PLACE OF BIRTH   Bangkok, Thailand

INSTITUTIONS ATTENDED   Bachelor of Engineering in Georesources Engineering, Chulalongkorn University (2013-2017)

HOME ADDRESS   Bangbon district, Bangkok, Thailand 10150